

RECEIVED: January 24, 2023 ACCEPTED: May 8, 2023 PUBLISHED: May 17, 2023

Worldsheet traversable wormholes

Jan de Boer, a Viktor Jahnke, b Keun-Young Kim b and Juan F. Pedraza c

^a Institute for Theoretical Physics, University of Amsterdam, Amsterdam, The Netherlands

E-mail: j.deboer@uva.nl, viktorjahnke@gist.ac.kr, fortoe@gist.ac.kr, j.pedraza@csic.es

ABSTRACT: We construct worldsheet traversable wormholes by considering the effects of a double-trace deformation, $\delta \mathcal{L} \sim h \partial \phi_L \partial \phi_R$, coupling the endpoints of an open string in AdS space. The operator deforming the theory is irrelevant and makes the boundaries bend inward toward the IR. This effect, reminiscent of two-dimensional dilaton gravities, renders the teleportation protocol more efficient and facilitates the transfer of information between the members of the dual Bell pair. We compare our results with those obtained with the standard double-trace deformation, $\delta \mathcal{L} \sim h \phi_L \phi_R$, introduced by Gao, Jafferis and Wall.

Keywords: AdS-CFT Correspondence, 2D Gravity, Field Theories in Lower Dimensions

ARXIV EPRINT: 2211.13262

^bSchool of Physics and Chemistry, Gwangju Institute of Science and Technology, Gwangju, Korea

^cInstituto de Física Teórica UAM/CSIC, Calle Nicolás Cabrera 13-15, Madrid 28049, Spain

Contents

1	Introduction $ \begin{array}{c} \text{Preliminaries: open strings and } \mathbf{AdS_2}/\mathbf{CFT_1} \end{array} $			1
2				4
	2.1	Class	ical string solutions and worldsheet black holes	4
	2.2	Semi-	classical worldsheet theory	(
		2.2.1	Two- and four-point functions	
3	Making worldsheet traversable wormholes			9
	3.1	Intro	ducing a double trace deformation	9
	3.2 Condition for traversability			10
	3.3	.3 Wormhole opening		12
	3.4	3.4 Two-sided commutator		18
		3.4.1	Going beyond the probe approximation	25
		3.4.2	Irrelevant deformations and imprint on the UV	24
4	Dis	cussio	n	30

1 Introduction

The landscape of spacetimes that could emerge from Einstein's field equations began to take on a variety of novel configurations not long after general relativity was discovered. A noteworthy example is a solution discovered in the mid '30s by Einstein himself and Rosen, describing a bridge between worlds, and known thereafter under the name of Einstein-Rosen bridge [1]. An Einstein-Rosen bridge is a vacuum solution to Einstein's equations that link two otherwise spatially disconnected spacetimes, what in modern terminology is referred to as a maximally extended Schwarzschild solution. Many generalizations have appeared since, including bridges connecting distant but causally connected regions of the same geometry and, thus, representing actual shortcuts in spacetime. These solutions were popularized after a seminal paper by Misner and Wheeler in the late '50s [2], which coined the term wormholes.

A crucial property of these wormholes is that energy-violating matter is typically needed to support their throats, which makes them seem to belong only in science fiction. However, recent progress has shown that these violations may naturally occur in quantum mechanics, suggesting that real-world traversable wormholes might exist. This raises fascinating questions about their nature and phenomenology, with some even proposing that they may be created in a laboratory, and use them in experiments of quantum teleportation [3, 4].

The interest in wormhole solutions was reignited with the discovery of the AdS/CFT correspondence [5], a robust framework that allows us to pose questions about quantum gravity and reformulate them in the language of field theory. In this context, a maximally extended or two-sided AdS black hole is known to map to the canonical purification of the thermal density matrix, known as the thermofield double state [6]. This unique, maximally entangled state is thus represented by an Einstein-Rosen bridge embedded in AdS space, leading to one of the central theses of the AdS/CFT correspondence, namely, the fact that entanglement generates connectivity in the bulk spacetime [7]. The ER=EPR correspondence, which connects EPR-type entanglement in boundary theory with the presence of an Einstein-Rosen bridge in dual bulk spacetime, provides a qualitative yet catchy formulation of this claim. Evidence for this correspondence includes [9–13], showing that single Bell pairs in the field theory (EPR or Hawking) can be thought of as generating Planckian-size wormholes, holographically represented by strings in AdS with an Einstein-Rosen bridge in the induced geometry.

Einstein-Rosen bridges in AdS are, however, not traversable. This is consistent with the fact that while entangled, the theories in the thermofield double state do not interact. Traversable wormholes, on the other hand, require a violation of the so-called Average Null Energy Condition (ANEC). For a local quantum field theory, the ANEC states that the integral of the stress-energy tensor along a complete achronal null geodesic is non-negative

$$\int T_{\mu\nu}k^{\mu}k^{\nu}d\lambda \ge 0, \qquad (1.1)$$

where k^{μ} is the tangent vector and λ is an affine parameter. Classically, a violation of ANEC is prevented by the Null energy Condition (NEC), $T_{\mu\nu}k^{\mu}k^{\nu} \geq 0$, which must be valid for any physically reasonable theory, and implies (1.1). However, quantum mechanical effects may induce negative null energy, leading to violations of the NEC and the ANEC. A prototypical example where such violations may be triggered was studied by Gao, Jafferis and Wall (GJW) [21], which showed that a double trace deformation of the form

$$\delta H = \int dx \, h(t, x) \, \mathcal{O}_L(-t, x) \, \mathcal{O}_R(t, x) \,, \qquad (1.2)$$

introduces the negative null energy in the bulk necessary to sustain a traversable wormhole.¹ They worked within the semi-classical approximation, where matter fields are treated quantum mechanically, but the gravitational field, or the metric, is treated classically. In this context, one is to solve the semi-classical Einstein's equations

$$G_{\mu\nu} = 8\pi G_N \langle T_{\mu\nu} \rangle \,, \tag{1.3}$$

where $G_{\mu\nu}$ is Einstein's tensor, and $\langle T_{\mu\nu} \rangle$ is the expectation value of the stress-energy tensor in a given quantum state. GJW showed that for certain choices of the coupling h(t,x), the 1-loop expectation value of the stress-energy tensor does indeed lead to

$$\int \langle T_{\mu\nu} \rangle k^{\mu} k^{\nu} d\lambda < 0, \qquad (1.4)$$

¹Technically, however, the coupling (1.2) breaks one of the assumptions of the proof of ANEC, since it is non-local. This deformation renders all null geodesics connecting the two sides of an eternal AdS black hole *non-achronal*.

rendering an Einstein-Rosen bridge traversable. This allows the transfer of information between the two asymptotic boundaries, a process that can be viewed as a teleportation protocol [21]. GJW considered the specific case of a two-sided BTZ black hole, but their construction was subsequently extended in several directions, for example, to black holes solutions in JT gravity [23–25], higher-dimensional black holes [26–28], asymptotically flat black holes [29], multi-boundary traversable wormholes [30, 31], eternal traversable wormholes [32–34], near-extremal black holes [35], and rotating black holes [36]. Other interesting developments include for instance [37–52]. For a recent review of wormholes in holography, see [53].

The stringy setups considered in [9–13], holographically dual to single entangled Bell pairs in the field theory, provide a natural and interesting environment where these ideas may be investigated. Indeed, the worldsheet theory of a string may be viewed as the simplest theory of 'quantum gravity' that one can solve [54]. Even though worldsheet theories do not contain explicit gravitational degrees of freedom, it is important to remember that they have several surprising qualities that are similar to gravity, including the absence of local off-shell observables, a minimal length, a maximum achievable Hagedorn temperature [54]. Further, their spectrum includes (integrable relatives of) black holes, which display fast scrambling and maximal chaos [55, 56]. This is evident from the fact that their low energy effective action includes a soft sector governed by a Schwarzian action which couples with other modes in the infrared [57–59], reminiscent of two-dimensional dilaton theories and the SYK model. Finally, in some cases worldsheet theories may be cast as $T\bar{T}$ -deformed field theories [60–62], which have proved crucial for studies of holography at a finite cutoff, e.g., [63–65].

This paper is organized as follows. We begin in section 2 with a quick review of open strings on AdS and the holographic dictionary for the worldsheet theory. Focusing on string states with an induced two-sided AdS₂ black hole geometry, we then discuss the computation of correlation functions using the extrapolate dictionary and sketch the derivation of two- and four-point functions, appearing in previous literature. In section 3 we consider the effects of a deformation that may naturally arise from interactions between the endpoints of the string. At the lowest order, this coupling is of the form $\delta \mathcal{L} \sim h \partial \phi_L \partial \phi_R$, in contrast with the standard deformation $\delta \mathcal{L} \sim h \phi_L \phi_R$ studied by Gao, Jafferis and Wall [21]. The effects of this deformation are studied in detail from the worldsheet perspective, drawing a comparison to the standard case that was considered in earlier research on AdS₂ holography [23].² The string coupling is irrelevant in the dual CFT₁ and, as expected from scaling arguments, does not lead to a large effect in the IR other than slightly opening the wormhole throat. However, the coupling induces a large backreaction in the UV, effectively pulling the AdS boundaries inward. This effect ultimately improves the bound on information transfer between one boundary to another, effectively rendering the teleportation protocol more efficient. We close in section 4 with a discussion of our results and open questions that remain for future work.

²It is also tempting to speculate about the boundary dual of such deformation. Qualitatively, we expect it should act similarly to a deformation of the type $\delta \mathcal{L} \sim hT_L\bar{T}_R$, recently considered in [66].

2 Preliminaries: open strings and AdS_2/CFT_1

2.1 Classical string solutions and worldsheet black holes

Let us start by describing our holographic setup. We will consider a generic bulk geometry of the form $\mathrm{AdS}_{d+1} \times X^p$, dual to some d-dimensional large- N_c field theory. We then consider a stack of N_f flavor branes on top of this geometry, with $N_f \ll N_c$. In this limit, the flavor branes act as probe branes and one may neglect their backreaction. The flavor branes will be assumed to span all directions of the dual theory, however, they will have compact radial support, spanning from boundary z=0 up to some cutoff surface z_c , where they end smoothly (meaning that one of their internal cycles shrinks down to zero size). A prototypical example is the standard D3/D7 system [67], however, will be largely agnostic about the precise details of the top-down construction.

We then consider a fundamental open string in such AdS space, with its two endpoints attached to one of the flavor branes.³ The dynamics of the string are governed by the standard Nambu-Goto action,

$$S_{\rm NG} = -\frac{1}{2\pi\alpha'} \int_{\Sigma} \sqrt{-\det \gamma_{\alpha\beta}} , \qquad (2.1)$$

where $\gamma_{\alpha\beta} = g_{\mu\nu}\partial_{\alpha}X^{\mu}\partial_{\beta}X^{\nu}$ is the induced metric on the worldsheet and $X^{\mu}(\tau,\sigma)$ are the embedding functions into the target space.

We will now consider global AdS_3 for concreteness, but the generalization to higher dimensions is straighforard. The bulk metric reads

$$ds^{2} = -\left(1 + \frac{\rho^{2}}{\ell^{2}}\right)d\tau^{2} + \rho^{2}d\varphi^{2} + \frac{d\rho^{2}}{\left(1 + \frac{\rho^{2}}{\ell^{2}}\right)}.$$
 (2.2)

It can be checked that a static string lying at a fixed azimuthal angle,

$$X^{\mu}(\tau, \rho) = \{\tau, \varphi(\tau, \rho) = \text{constant}, \rho\}, \qquad (2.3)$$

solves the equations of motion and is therefore a valid solution. This situation is depicted in figure 1. One may wonder how this solution looks like from the point of view of a Poincaré observer, which only has access to part of the spacetime — see figure 1 for an illustration. The bulk metric in this case takes the form

$$ds^{2} = \frac{\ell^{2}}{u^{2}} \left[-d\mathbf{t}^{2} + d\mathbf{x}^{2} + du^{2} \right], \qquad (2.4)$$

and the string profile maps to the well-known solution with constant acceleration [14, 15],

$$X^{\mu}(\mathbf{t}, u) = \{\mathbf{t}, \mathbf{x}(\mathbf{t}, u) = \sqrt{A^{-2} + \mathbf{t}^2 - u^2}, u\}.$$
 (2.5)

This profile is shown in figure 2. The accelerated solution contains a two-sided horizon and a wormhole in the induced worldsheet geometry [11]. As pointed out in this paper, one may

³The string is dual to a pair of infinitely heavy quarks in the limit $z_c \to 0$. Finite z_c introduces a scale that can be associated with the mass of the quarks [67].

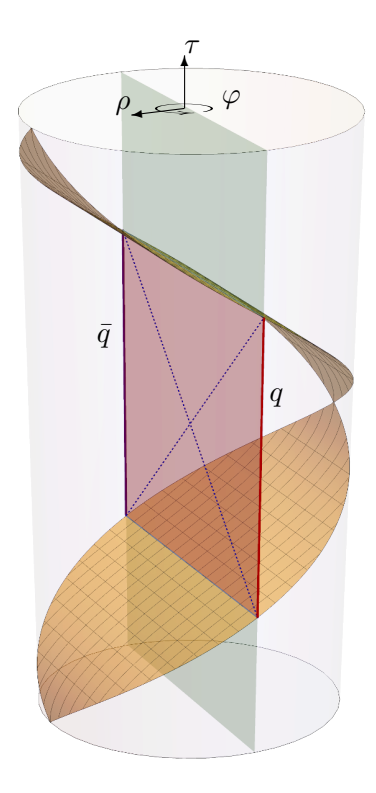


Figure 1. Static string dual to a quark q and anti-quark \bar{q} pair in global AdS. The two null planes depicted in yellow delimit the interior of a Poincaré patch, as seen by an accelerated observer. From the point of view of this Poincaré observer, the $q\bar{q}$ -pair undergoes back-to-back constant acceleration. The induced worldsheet geometry hence includes a two-sided horizon and a wormhole, which is classically non-traversable.

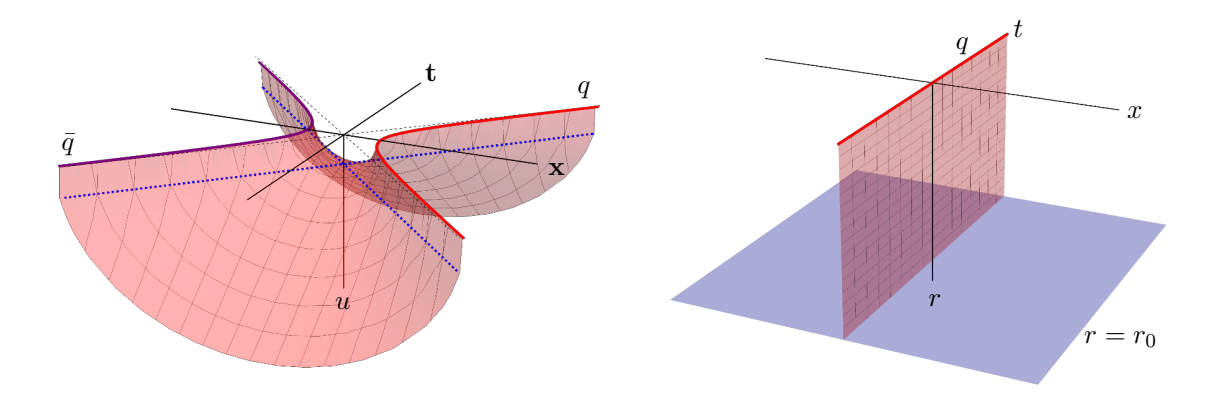


Figure 2. Left: uniformly-accelerated quark-anti-quark pair $(q\bar{q})$ and their corresponding string dual, plotted in the Poincaré patch of AdS. The worldsheet geometry includes a two-sided horizon and a wormhole, which is classically non-traversable. Right: string embedding in a Rindler patch of AdS. This coordinate system only covers one side of the solution, corresponding to one of the quarks. The solution is static and stretches between the boundary of AdS and an accelerating horizon that develops in the bulk.

deform this solution in a number of ways (as allowed by the classical equations of motion) but always in a way such that the corresponding wormhole remains *non-traversable*.

One can further specialize to the case of a Rindler observer in the bulk, in which case, only part of the string embedding is accessible. The bulk metric in this case takes the form of a (planar) BTZ black brane

$$ds^{2} = -r^{2}f(r)dt^{2} + r^{2}dx^{2} + \frac{dr^{2}}{r^{2}f(r)}, \qquad f(r) = 1 - \left(\frac{r_{0}}{r}\right)^{2}, \qquad (2.6)$$

and the embedding corresponds to a static vertical string that stretches between the AdS boundary and the horizon [16]

$$X^{\mu}(t,r) = \{t, x(t,r) = 0, r\}. \tag{2.7}$$

The induced metric on the worldsheet takes the form of a 2d black hole:

$$\gamma_{\alpha\beta} = \begin{pmatrix} -r^2 f(r) & 0\\ 0 & \frac{1}{r^2 f(r)} \end{pmatrix},\tag{2.8}$$

which coincides with a constant-x section of a BTZ black brane. Perturbations over the static string embedding thus correspond to perturbations on top of this 2d black hole. Since black holes are known to be fast scramblers and saturate the bound on the quantum Lyapunov exponent λ_L , this lead to the conjecture that open strings could also exhibit maximal chaos. Indeed, explicit calculation of the four-point OTOC [56] confirmed this intuition.

2.2 Semi-classical worldsheet theory

The worldsheet theory for fluctuations around the static string embedding can be understood as a QFT living on a black hole background. To see the details of this theory, we can expand the NG action around this solution, i.e., $X^{\mu} = X_0^{\mu} + \delta X^{\mu}$, where

$$X_0^{\mu}(t,r) = \{t, x(t,r) = 0, r\}, \qquad \delta X^{\mu}(t,r) = \{0, \delta x(t,r) \equiv \phi(t,r), 0\}.$$
 (2.9)

Plugging this into the action we obtain:

$$S = S_{\text{free}} + S_{\text{int}} \,, \tag{2.10}$$

where S_{free} is the action of the free theory and S_{int} is the interaction piece, respectively:

$$S_{\text{free}} = \frac{1}{2} \int dt dr \left(\frac{\dot{\phi}^2}{f} - r^4 f \phi'^2 \right), \qquad S_{\text{int}} = \frac{\kappa}{4} \int dt dr \left(\frac{\dot{\phi}^2}{f} - r^4 f \phi'^2 \right)^2 + \cdots. \tag{2.11}$$

For convenience, we have rescaled $\phi \to \sqrt{2\pi\alpha'}\phi$ and set $\kappa = \pi\alpha'$. Also, notice that we have only included interactions up to quartic order, which are relevant for the calculation of two- and four-point functions at leading order in α' . In the next subsection, we will review the calculation of these correlators using the well-known 'extrapolate' prescription.

2.2.1 Two- and four-point functions

The equation of motion that follows from S_{free} is:

$$[-f^{-1}\partial_t^2 + \partial_r(r^4f\partial_r)]\phi(t,r) = 0 \qquad \to \qquad [f^{-1}\omega^2 + \partial_r(r^4f\partial_r)]g(r) = 0, \qquad (2.12)$$

where we have set $\phi(t,r) = e^{-i\omega t}g(r)$. The two linearly independent solutions to this equation can be written as $g_{\pm\omega}(r)$ where:

$$g_{\omega}(r) = \frac{1}{1+i\nu} \frac{\rho+i\nu}{\rho} \left(\frac{\rho-1}{\rho+1}\right)^{i\nu/2}, \qquad (2.13)$$

and we have defined the following dimensionless variables:

$$\rho \equiv \frac{r}{r_0}, \qquad \nu \equiv \frac{\omega}{r_0} = \frac{\beta \omega}{2\pi}. \tag{2.14}$$

These solutions satisfy $g_{\omega}(r)^* = g_{-\omega}(r)$ and are purely outgoing/ingoing, respectively. To see this, we can define the tortoise coordinate r_* such that

$$dr_*^2 = \frac{dr^2}{r^4 f(r)^2} \,. \tag{2.15}$$

This coordinate is convenient because the worldsheet metric becomes conformally flat and the fluctuations are easier to analyze. Integrating (2.15) we find

$$r_* = -\frac{1}{r_0}\operatorname{arccoth}\left(\frac{r}{r_0}\right). \tag{2.16}$$

As we can see, the horizon is mapped to $r_* \to -\infty$ while the boundary is now at $r_* \to 0$. In particular, in the near-horizon region, we have

$$r_* \sim \frac{1}{2r_0} \log \left(\frac{r}{r_0} - 1\right) \,,$$
 (2.17)

and the equation of motion becomes

$$(\omega^2 + \partial_{r_*}^2)g(r) \approx 0. (2.18)$$

It is easy to see that the solutions should take the following form:

$$g(r) \approx e^{i\omega r_*}$$
 (outgoing), $g(r) \approx e^{-i\omega r_*}$ (ingoing). (2.19)

In terms of the tortoise coordinate, (2.13) becomes:

$$g_{\omega}(r) = \frac{1}{1+i\nu} \frac{\rho + i\nu}{\rho} e^{i\omega r_*}, \qquad (2.20)$$

so we can indeed identify $g_{\pm\omega}(r)$ as outgoing/ingoing solutions. Next, we impose a Neumann boundary condition for $\phi(r,t)$ in the UV,⁴

$$\partial_r \phi(r_c, t) = 0, \qquad (2.21)$$

⁴Normally, one would choose normalizable boundary conditions in the UV. However, that would correspond to a string extending all the way to the AdS boundary. The mass of the dual particles would be infinite and the correlators would trivially vanish. Instead, we introduce a UV cutoff r_c to make the masses finite and allow for string fluctuations in the UV. We implement this by means of a Neumann boundary condition at $r = r_c$.

where $r_c = 1/z_c$ is a UV cutoff. This condition dictates that we take the linear combination:

$$f_{\omega}(r) = g_{\omega}(r) + e^{i\theta_{\omega}} g_{-\omega}(r), \qquad e^{i\theta_{\omega}} = -\frac{\partial_r g_{\omega}(r_c)}{\partial_r g_{-\omega}(r_c)}.$$
 (2.22)

It is easy to see that the phase θ_{ω} is real. The field ϕ can now be expanded as follows:

$$\phi(t,r) = \frac{\sqrt{2\pi\alpha'}}{r_H} \int_0^\infty \frac{d\omega}{2\pi} \frac{1}{\sqrt{2\omega}} \left[f_\omega(r) e^{-i\omega t} a_\omega + f_\omega(r)^* e^{i\omega t} a_\omega^{\dagger} \right], \tag{2.23}$$

The normalization constant in front of (2.23) appears after properly normalizing the mode functions $f_{\omega}(r)$ [17]. Moreover, since the system is at finite temperature T, the expectation value of the creation and annihilation operators should follow a Bose distribution:

$$\langle a_{\omega}^{\dagger} a_{\omega'} \rangle = \frac{2\pi\delta(\omega - \omega')}{e^{\beta\omega} - 1} \,. \tag{2.24}$$

We will be interested in the Wightman and retarded propagators, defined as follows:

$$D_W(t - t', r, r') = \langle \phi(t, r)\phi(t', r') \rangle,$$

$$D_{\text{ret}}(t - t', r, r') = \theta(t - t')\langle [\phi(t, r), \phi(t', r')] \rangle.$$
(2.25)

Using the wave equation (2.12) and the canonical commutation relation

$$[\phi(t,r),\dot{\phi}(t,r')] = 2\pi i\alpha' f\delta(r-r'), \qquad (2.26)$$

it can be shown that these propagators satisfy

$$[-f^{-1}\partial_t^2 + \partial_r(r^4 f \partial_r)]D_W(t - t', r, r') = 0, \qquad (2.27)$$

$$[-f^{-1}\partial_t^2 + \partial_r(r^4 f \partial_r)]D_{\text{ret}}(t - t', r, r') = 2\pi i \alpha' \delta(t - t')\delta(r - r'). \qquad (2.28)$$

It is then easy to show that the Wightman propagator can be written as

$$D_W(\omega, r, r') = \frac{2\pi\alpha'}{r_0^2} \frac{f_\omega(r)f_{-\omega}(r')}{2\omega(1 - e^{-\beta\omega})},$$
(2.29)

where $f_{-\omega} = f_{\omega}^*$. These correlators can also be derived using the Schwinger-Keldysh path integral formalism [18].

Depending on time ordering, there are a few possible four-point correlation functions that will be of interest to our purposes. These can be written as

$$D(t_1, t_2, t_3, t_4) = \langle W(t_1)V(t_2)W(t_3)V(t_4)\rangle. \tag{2.30}$$

In this case, one may consider the standard Schwinger-Keldysh contour or a more general time-fold to obtain exotic time orderings (see e.g. [19]). The relevant one to study chaos is the out-of-time-order (OTOC) for which $t_1 > t_2$ and $t_3 > t_4$ but $t_2 < t_3$ and $t_4 < t_1$. This correlator was studied in [56] for the case at hand. The OTOC calculation boils down to computing a scattering amplitude in the near-horizon region, which may be obtained using the eikonal approximation. This gives the following result [19]

$$D_{\text{otoc}}(t_1, t_2, t_3, t_4) = \int_0^\infty dp \, \psi_1(p) \psi_3^*(p) \int_0^\infty dq \, \psi_2(q) \psi_4^*(q) \, e^{i\delta} \,, \tag{2.31}$$

where the wave functions ψ_i are Fourier transforms of bulk-to-boundary correlators

$$\psi_1(p) = \int dv e^{2ipv} \langle \varphi_V(u, v) V(t_1)^{\dagger} \rangle \big|_{u=0}, \qquad (2.32)$$

$$\psi_2(q) = \int du e^{2ipu} \langle \varphi_W(u, v) V(t_2)^{\dagger} \rangle \big|_{v=0}, \qquad (2.33)$$

$$\psi_3(p) = \int dv e^{2ipv} \langle \varphi_V(u, v) V(t_3) \rangle \big|_{u=0}, \qquad (2.34)$$

$$\psi_4(q) = \int du e^{2ipu} \langle \varphi_W(u, v) V(t_4) \rangle \big|_{v=0}, \qquad (2.35)$$

 φ_V and φ_W are the worldsheet fields dual to the boundary operators V and W, and u and v are Kruskal coordinates (see (3.5)). The phase shift is given by

$$\delta(s) = \frac{s\ell_s^2}{4} \,, \tag{2.36}$$

where $s = (\Delta E)^2$ is the standard Mandelstam variable and $\ell_s \equiv \sqrt{2\pi\alpha'}$. Evaluating (2.30) at leading order in ℓ_s^2 for $t_1 = i\epsilon_1, t_2 = t + i\epsilon_2, t_3 = i\epsilon_3$ and $t_4 = t + i\epsilon_4$, and normalizing the correlator with respect to the leading order term, one finds [56]

$$\frac{\langle V(i\epsilon_1)W(t+i\epsilon_2)V(i\epsilon_3)W(t+i\epsilon_4)\rangle}{\langle V(i\epsilon_1)V(i\epsilon_3)\rangle\langle W(t+i\epsilon_2)W(t+i\epsilon_4)\rangle} = 1 + \frac{2i\ell_s^2}{\epsilon_{13}\epsilon_{24}^*}e^{2\pi Tt}, \qquad (2.37)$$

where $\epsilon_{mn} = i \left(e^{i2\pi T \epsilon_m} - e^{i2\pi T \epsilon_n} \right)$. From (2.37) we can read off the Lyapunov exponent $\lambda_L = 2\pi T$, which saturates the chaos bound [20].

3 Making worldsheet traversable wormholes

3.1 Introducing a double trace deformation

Following the seminal work of Gao, Jafferis and Wall [21], one may wonder if we can consider the effects of a non-local coupling to construct traversable wormholes in the worldsheet. In order to do so, we must first ask what the natural form of such a coupling may be. To start with, we note that each endpoint of the string can be coupled to a flavor brane via the boundary term (see e.g. [22])

$$S_F = \int_{\partial \Sigma} A_\mu \dot{X}^\mu \,. \tag{3.1}$$

Normally, A_{μ} is meant to be taken as an external field on the brane, which one can turn on by hand. However, in our context, it is natural to take inspiration from the form of the backreacted field that arises from the presence of the second endpoint of the string. For a point-like source, this field is expected to follow the standard Liénard-Wiechert form, $A_{\mu} \sim \delta \dot{X}_{\mu}$. In our conventions (2.9), then, we are then led to consider a coupling of the form:⁵

$$S_F = h \int_{\partial \Sigma} \dot{\phi}_L \dot{\phi}_R \,, \tag{3.2}$$

⁵The form of the potential $A_{\mu} \sim \delta \dot{X}_{\mu}$ could also be justified since this is the only choice that makes S_F symmetric between the left and right boundaries/endpoints of the string.

where h is a parameter that controls the strength of the backreaction. This is a bilocal coupling, as in [21], but involving derivatives. It is important to emphasize that backreaction itself is not enough to obtain such a coupling, as (3.2) requires to properly account for retarded times and, hence, cannot possibly be instantaneous. Nevertheless, terms like (3.2) are quite natural to describe the leading interactions between endpoints since it is $\partial \phi$, and not ϕ , that represents a primary operator from the worldsheet perspective. In the following, we will thus proceed by assuming that such a coupling has been turned on and study its implications.

To construct the traversable wormhole it would suffice to consider the free theory S_{free} (free massless scalar field) together with the non-local coupling (3.2), i.e., one can ignore the higher order interactions in a first approximation. However, the interaction terms in S_{int} are important in order to actually study the information transfer, as one must take them into account for the computation of four- and higher-point correlators.

One difference between our work and the standard setup considered by Gao, Jafferis and Wall [21] is that our worldsheet metric $\gamma_{\alpha\beta}$ does not satisfy the semiclassical Einstein equation,

$$R_{\alpha\beta} - \frac{1}{2}R\gamma_{\alpha\beta} + \Lambda\gamma_{\alpha\beta} = \langle T_{\alpha\beta} \rangle, \qquad (3.3)$$

or its equivalent in 2d dilaton gravity. Instead, it satisfies the (perhaps simpler) semiclassical equation

$$\gamma_{\alpha\beta} = g_{\mu\nu} \langle \partial_{\alpha} X^{\mu} \partial_{\beta} X^{\nu} \rangle \,. \tag{3.4}$$

3.2 Condition for traversability

To understand the conditions under which the worldsheet wormhole becomes traversable, it is convenient to use Kruskal coordinates (u, v):

$$e^{2r_0t} = -\frac{u}{v}, \quad \frac{r}{r_0} = \frac{1-uv}{1+uv},$$
 (3.5)

and parametrize the embedding as $X^{\mu} = (u, v, X(u, v))$, which corresponds to a string stretching between the two asymptotic boundaries of an eternal AdS black hole. Considering a static solution X(u, v) = 0, the worldsheet metric can be written as

$$ds_{\rm ws}^2 = -\frac{4dudv}{(1+uv)^2} \,. \tag{3.6}$$

The corresponding Penrose diagram is shown in figure 3.

We note that a null ray originating from the left asymptotic boundary and moving along the v=0 horizon reaches the future singularity, never crossing to the right exterior region. One might wonder whether fluctuations of the geometry (3.6) induced by string fluctuations can lead to a traversable wormhole. To analyze this, we start by parameterizing the string worldsheet with null coordinates (u, v) and consider perturbations $\delta x(u, v) = \phi(u, v)$ around the static solution. In this case, the worldsheet metric (3.6) becomes

$$ds^{2} = -\frac{4dudv}{(1+uv)^{2}} + \bar{\gamma}_{\alpha\beta}dx^{\alpha}dx^{\beta}, \qquad (3.7)$$

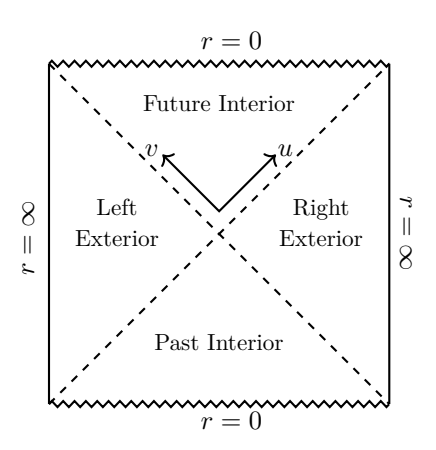


Figure 3. Penrose diagram for the eternal AdS black hole described by (3.6). In our conventions, time increases as one goes up (down) along the right (left) asymptotic boundary.

where

$$\bar{\gamma}_{\alpha\beta} = g_{xx} \langle \partial_{\alpha} \phi \partial_{\beta} \phi \rangle . \tag{3.8}$$

Next, we consider a perturbation moving in the v direction and take $\phi(u, v) = F(u)$, where F(u) is assumed to vanish outside a window around $u = u_0$. It is easy to check that only $\bar{\gamma}_{uu}$ is non-zero, and is given by

$$\bar{\gamma}_{uu} = \left(\frac{1 - uv}{1 + uv}\right)^2 F'(u)^2. \tag{3.9}$$

We can now determine how the above perturbation changes the trajectory of a null ray originating from the left asymptotic boundary and moving along the v = 0 horizon. Let u be the affine parameter along this ray. Along the trajectory of the ray, we have

$$\left[-\frac{4dudv}{(1+uv)^2} + \left(\frac{1-uv}{1+uv}\right)^2 F'(u)^2 du^2 \right]_{v=0} = 0,$$
 (3.10)

which implies

$$dv = \frac{F'(u)^2}{4} du \,. \tag{3.11}$$

By integrating (3.11), we find that the null shift that the ray suffers as it crosses the perturbation at $u = u_0$ is given by

$$\Delta v(u) = \frac{1}{4} \int_{-\infty}^{u} F'(u)^2 du.$$
 (3.12)

Note that Δv may be related to the energy of the perturbation, which is given by [56]

$$\Delta E = 2 \int du F'(u)^2. \tag{3.13}$$

Therefore

$$\Delta v = \frac{\Delta E}{8} \,. \tag{3.14}$$

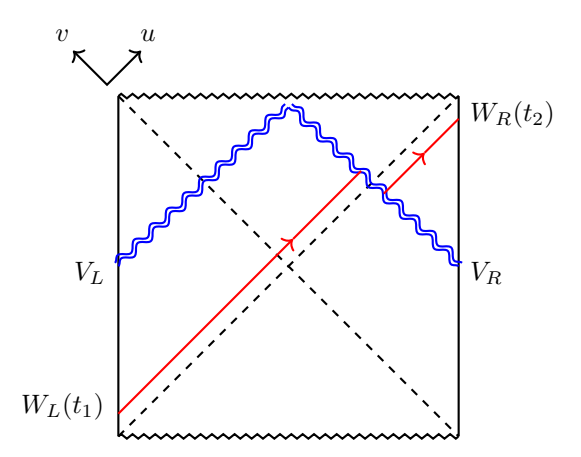


Figure 4. The non-local coupling between V_L and V_R introduces a negative-energy shock wave in the bulk that makes the wormhole traversable. The traversability can be diagnosed by a two-sided correlation function involving W_L and W_R .

The worldsheet wormhole becomes traversable if $\Delta v < 0$, which implies $\Delta E < 0$, i.e., the traversability requires the presence of a perturbation with negative energy. Of course, negative energy is forbidden for classical perturbations and so are worldsheet traversable wormholes [11]. This condition is analogous to the so-called Average Null Energy Condition (ANEC), which needs to be overcome for wormhole traversability to be possible. In the next subsection, we will see that quantum effects in the worldsheet, together with the double trace coupling (3.2), may indeed lead to a configuration where traversability is allowed.

3.3 Wormhole opening

Inspired by [21], we now compute the opening of the wormhole using a point-splitting technique. We start with the semiclassical equation

$$\gamma_{\alpha_{\beta}} = g_{\mu\nu} \langle \partial_{\alpha} X^{\mu} \partial_{\beta} X^{\nu} \rangle , \qquad (3.15)$$

and its fluctuation version (3.8), from which we can obtain the opening of the wormhole as

$$\Delta v(u) = -\frac{1}{2\gamma_{uv}(0)} \int_{-\infty}^{u} \bar{\gamma}_{uu} du. \qquad (3.16)$$

In the point splitting method, we can compute the metric perturbation (3.6) as

$$\bar{\gamma}_{\alpha\beta} = \lim_{\sigma' \to \sigma} \partial_{\alpha} \partial_{\beta}' G(\sigma, \sigma') , \qquad (3.17)$$

where $\sigma = (u, v)$ and $\sigma' = (u', v')$ denote worldsheet points, and $G(\sigma, \sigma')$ is a renormalized two-point function under the presence of a Hamiltonian deformation $\delta H(t)$:

$$G(u, v; u', v') = g_{xx} \langle \phi_H(u, v) \phi_H(u', v') \rangle = g_{xx} \langle \phi_H(t, r) \phi_H(t', r') \rangle,$$

= $g_{xx} \langle U^{-1}(t, t_0) \phi_I(t, r) U(t, t_0) U^{-1}(t', t_0) \phi_I(t', r') U(t', t_0) \rangle,$ (3.18)

where $U(t, t_0) = \mathcal{T}e^{-i\int_{t_0}^t dt \delta H(t)}$ denotes the evolution operator in the interaction picture, while $g_{xx} = \frac{(1-uv)^2}{(1+uv)^2}$. The subscripts H and I in the first and second lines of (3.18) indicate

a field in the Heisenberg and interaction pictures, respectively. In what follows, we will suppress the subscript I. Further, we will consider fields in the right exterior region of the geometry.

We are interested in the uu component of the worldsheet metric, which only involves derivatives of G(u, v; u', v') with respect to u and u'. This leads to the following simplification

$$\bar{\gamma}_{uu} = \lim_{(u',v')\to(u,v)} \partial_u \partial_{u'} G(u,v;u',v') = \lim_{u'\to u} \partial_u \partial_{u'} G(u,v;u',v). \tag{3.19}$$

Moreover, we only focus on $\bar{\gamma}_{uu}$ on the horizon v=0, which leads to

$$\bar{\gamma}_{uu} = \lim_{u' \to u} \partial_u \partial_{u'} G(u, 0; u', 0). \tag{3.20}$$

Therefore, we only need to care about G(u,0;u',0). Note that, by taking v=v'=0 in (3.18) we obtain

$$G(u,0;u',0) = \langle U^{-1}\phi(u,0)UU^{-1}\phi(u',0)U\rangle.$$
(3.21)

We now compute G(u, 0; u', 0) at first order in perturbation theory. We perform an expansion for small h and write the two-point function $G(\sigma, \sigma')$ as

$$G(\sigma, \sigma') = G_0(\sigma, \sigma') + G_h(\sigma, \sigma') h + \cdots, \qquad (3.22)$$

where G_0 is the unperturbed two-point function, while G_h corresponds to the first correction induced by the deformation δH . Using (3.18), we can see that

$$G_h = -i \int_{t_0}^t dt_1 \langle [\phi(t, r), \delta H(t_1)] \phi(t', r') \rangle - i \int_{t_0}^{t'} dt_1 \langle \phi(t, r) [\phi(t', r'), \delta H(t_1)] \rangle.$$
 (3.23)

Now we need to specify the deformation δH . We are going to consider two cases:

• Case I:

$$\delta H(t) = h(t) \phi_L(-t)\phi_R(t) \text{ with } h(t) = h\left(\frac{2\pi}{\beta}\right)^{1-2\Delta} \theta\left(\frac{2\pi}{\beta}(t-t_0)\right), \quad (3.24)$$

and

• Case II:

$$\delta H(t) = h(t)\dot{\phi}_L(-t)\dot{\phi}_R(t) \text{ with } h(t) = h\left(\frac{2\pi}{\beta}\right)^{-1-2\Delta} \theta\left(\frac{2\pi}{\beta}(t-t_0)\right), \quad (3.25)$$

where $\beta = \frac{2\pi\ell^2}{r_0}$ is the inverse temperature. The scaling factors $(\frac{2\pi}{\beta})^{1-2\Delta}$ and $(\frac{2\pi}{\beta})^{-1-2\Delta}$ are introduced here for convenience, to make h dimensionless.

In the remaining of this section, we will set $r_0 = \ell = 1$ to lighten the notation, but they could be easily restored. The results for general values of r_0 can be found in section 3.4. Further, we point out that the effects of the coupling I have been studied and reported in previous literature, originally in [21] for d = 2 and in [40] for arbitrary d (our case corresponds to d = 1). We include the analysis of this coupling here for completeness.

Case I: $\delta H(t) = h(t) \phi_L(-t) \phi_R(t)$. In this case, we obtain⁶

$$iG_{h} = \int_{t_{0}}^{t} dt_{1}h(t_{1})\langle [\phi(t,r),\phi_{L}(-t_{1})\phi_{R}(t_{1})]\phi(t',r')\rangle +$$

$$+ \int_{t_{0}}^{t'} dt_{1}h(t_{1})\langle \phi(t,r)[\phi(t',r'),\phi_{L}(-t_{1})\phi_{R}(t_{1})]\rangle.$$
(3.26)

Factorizing the above four-point functions in terms of a product of two-point functions and using causality, we can write

$$G_h = -i \int_{t_0}^t dt_1 h(t_1) \langle \phi(t', r') \phi_L(-t_1) \rangle \langle [\phi(t, r), \phi_R(t_1)] \rangle + (t \leftrightarrow t').$$
 (3.27)

Note this expression is not invariant under $L \leftrightarrow R$ because there are two operator insertions on the left boundary. Next, we use the KMS condition [68]:

$$\langle \mathcal{O}_R(t)\mathcal{O}_L(t')\rangle_{\text{TFD}} = \langle \mathcal{O}_R(t)\mathcal{O}_R(t'+i\beta/2)\rangle_{\text{TFD}},$$
 (3.28)

and write the final result in terms of a product of bulk-to-boundary correlators

$$G_h = 2\sin(\pi\Delta) \int dt_1 h(t_1) K(t' + t_1 - i\beta/2, r') K^r(t - t_1, r) + (t \leftrightarrow t'), \qquad (3.29)$$

where

$$K(t - t', r) \equiv \langle \phi(t, r)\phi(t', \infty) \rangle, \qquad (3.30)$$

$$K^{r}(t-t',r) = |K(t-t',r)|\theta(t) \theta\left(\frac{\sqrt{r^{2}-r_{0}^{2}}}{r_{0}}\cosh(t-t') - \frac{r}{r_{0}}\right), \qquad (3.31)$$

denote the Wightman bulk-to-boundary propagator and the retarded bulk-to-boundary propagator, respectively. In AdS-Rindler coordinates (t,r), the bulk-to-boundary propagator for a scalar field dual to an operator of dimension Δ is

$$K_{\Delta}(t,r) = c_{\Delta} \left[-\frac{\sqrt{r^2 - r_0^2}}{r_0} \cosh(t - t') + \frac{r}{r_0} \right]^{-\Delta},$$
 (3.32)

where

$$c_{\Delta} = \frac{\Gamma(\Delta)}{2^{\Delta+1} \pi^{1/2} \Gamma(\Delta+1/2)}.$$
(3.33)

For convenience, we will do the calculations for a generic scalar field of dimension Δ and we will set $\Delta = 1$ at the end of our calculations. Furthermore, it is more convenient to use Kruskal coordinates (u, v), in which terms the propagator becomes

$$K_{\Delta}(u, v; u_1) = c_{\Delta} \left[\frac{1 + uv}{vu_1 - \frac{u}{u_1} + 1 - uv} \right]^{\Delta}.$$
 (3.34)

⁶We only need to consider the contribution from G_h because the contribution coming from G_0 is fixed by symmetry to be proportional to the background metric. Therefore, G_0 just leads to a rescaling of the AdS length scale, which does not contribute to the wormhole opening Δv . Also, note $G_h(\sigma, \sigma')$ is finite even for $\sigma = \sigma'$, so the point-splitting is not essential to compute this contribution.

Thus, evaluated at v = 0 in Kruskal coordinates, G_h becomes

$$G_h(u, u') = 2\ell_s^2 \sin(\pi \Delta) c_\Delta^2 \int \frac{du_1}{u_1} h(u_1) \frac{\theta\left(\frac{u}{u_1} - 1\right)}{\left(\frac{u}{u_1} - 1\right)^\Delta} \frac{1}{(u_1 u' + 1)^\Delta} + (u \leftrightarrow u')$$

$$\equiv H(u, u') + H(u', u), \tag{3.35}$$

where $u_1 = e^{r_0 t_1}$. Importantly, the above bulk-to-boundary propagators are appropriate for fluctuations with a canonical kinetic term, which is the case if we rescale the fluctuations as $\phi \to \ell_s \phi$ as in (2.11). This rescaling introduces a factor of ℓ_s^2 in G_h .

The uu component of the perturbed worldsheet metric is then computed as

$$\bar{\gamma}_{uu} = 2 h \lim_{u' \to u} \partial_u \partial_{u'} H(u, u'), \qquad (3.36)$$

where H(u, u') is defined in (3.35). Likewise, the wormhole opening (3.16) now reads

$$\Delta v = -\frac{1}{2\gamma_{uv}(0)} \int_{u_0}^u \bar{\gamma}_{uu} du = \frac{1}{4} \int_{u_0}^u du \, 2 \lim_{u' \to u} \partial_u \partial_{u'} H(u, u') \,, \tag{3.37}$$

$$= \frac{1}{2} \int_{u_0}^{u} \lim_{u' \to u} \partial_u \tilde{H}(u, u'; u_0), \qquad (3.38)$$

where

$$\tilde{H}(u, u'; u_0) \equiv \partial_{u'} H(u, u') = C_0 \int_{u_0}^u du_1 \frac{u_1^{\Delta}}{(u - u_1)^{\Delta} (u' u_1 + 1)^{\Delta + 1}}, \tag{3.39}$$

and with $C_0 = 2h\Delta \sin(\pi\Delta)c_{\Delta}^2$. Notice that

$$\lim_{u' \to u} \partial_u \tilde{H}(u, u'; u_0) = \partial_u \tilde{H}(u, u; u_0) - \partial_u^{(2)} \tilde{H}(u, u; u_0), \qquad (3.40)$$

where $\partial_u^{(2)}$ denotes a derivative that acts only on the second argument of $\tilde{H}(u, u; u_0)$. Using the above relation, we can write

$$\int_{u_0}^{\infty} \lim_{u' \to u} \partial_u \tilde{H}(u, u'; u_0) = \tilde{H}(\infty, \infty; u_0) - \tilde{H}(u_0, u_0; u_0) - \int_{u_0}^{\infty} du \, \partial_u^{(2)} \tilde{H}(u, u; u_0) \,. \quad (3.41)$$

Noticing that $\tilde{H}(\infty, \infty; u_0) = 0$ and $\tilde{H}(u_0, u_0; u_0) = 0$, we arrive at

$$\Delta v = -\frac{C_0}{2} \int_{u_0}^{\infty} du \, \partial_u^{(2)} \tilde{H}(u, u; u_0) = -\frac{C_0}{2} \int_{u_0}^{\infty} du \int_{u_0}^{u} du_1 \, \frac{(\Delta + 1)u_1^{\Delta + 1}}{(u - u_1)^{\Delta} (u u_1 + 1)^{\Delta + 2}} \,. \quad (3.42)$$

We now use the identity

$$\int_{u_0}^{\infty} du \int_{u_0}^{u} du_1 \, \mathcal{F}(u, u_1) = \int_{u_0}^{\infty} du_1 \int_{u_1}^{\infty} du \, \mathcal{F}(u, u_1) \,, \tag{3.43}$$

with $\mathcal{F}(u, u_1) = -\frac{C_0}{2} \frac{(\Delta+1)u_1^{\Delta+1}}{(u-u_1)^{\Delta}(uu_1+1)^{\Delta+2}}$, and write

$$\Delta v = -\frac{C_0}{2} \int_{u_0}^{\infty} du_1 u_1^{\Delta+1} \int_{u_1}^{\infty} du \, \frac{(\Delta+1)}{(u-u_1)^{\Delta} (uu_1+1)^{\Delta+2}} \,. \tag{3.44}$$

Defining $w = \frac{u-u_1}{u+u_1}$, and after some manipulations, (3.44) becomes

$$\Delta v = -\frac{(\Delta+1)C_0}{2^{\Delta}} \int_{u_0}^{\infty} du_1 u_1^2 \int_0^1 dw \, \frac{(1-w)^{2\Delta} w^{-\Delta}}{\left[1+u_1^2+(u_1^2-1)w\right]^{\Delta+2}},$$

$$= -\frac{(\Delta+1)C_0}{2} \frac{\Gamma(1-\Delta)\Gamma(1+2\Delta)}{\Gamma(\Delta+2)} \int_{u_0}^{\infty} du_1 \frac{u_1^{2\Delta}}{(1+u_1)^{2\Delta+1}}.$$
(3.45)

Next, we use the integral representation of the incomplete Beta function

$$\int_{u_0}^{\infty} du_1 \frac{u_1^{2\Delta}}{(1+u_1^2)^{2\Delta+1}} = -\frac{i(-1)^{-\Delta}}{2} B(-u_0^{-2}; \Delta + 1/2, -2\Delta), \qquad (3.46)$$

together with the following identities

$$B(x; a, b) = \frac{x^a}{a} {}_{2}F_1(a, 1 - b, a + 1; x), \qquad (3.47)$$

$$_{2}F_{1}(A,B,C;x) = (1-x)^{-A} {}_{2}F_{1}\left(A,C-B,C;\frac{x}{x-1}\right),$$
 (3.48)

$$\sin(\pi\Delta) = \frac{\pi}{\Gamma(1-\Delta)\Gamma(\Delta)}, \qquad (3.49)$$

to finally show that

$$\Delta v = -h\ell_s^2 \frac{\pi}{2\Delta + 1} \frac{\Gamma(2\Delta + 1)}{\Gamma(\Delta)^2} c_\Delta^2 \frac{{}_2F_1\left(\Delta + 1/2, 1/2 - \Delta, \Delta + 3/2, \frac{1}{1 + u_0^2}\right)}{(1 + u_0^2)^{\Delta + 1/2}}.$$
 (3.50)

The above result was obtained for $h(t) = h \theta(t - t_0)$ and $r_0 = 1$. For the case of a instantaneous perturbation, i.e., $h^{\text{inst}}(t) = h \delta(t - t_0)$, we obtain⁷

$$\Delta v^{\text{inst}} = -u_0 \partial_{u_0} \Delta v(u_0) = -\pi h \ell_s^2 \frac{\Gamma(2\Delta + 1)}{\Gamma(\Delta)^2} c_\Delta^2 \left(\frac{u_0}{1 + u_0^2}\right)^{2\Delta + 1} . \tag{3.51}$$

We recall that in the above formulas $u_0 = e^{t_0}$.

Case II: $\delta H(t) = h(t) \dot{\phi}_L(-t) \dot{\phi}_R(t)$. In this case, we obtain

$$G_h = 2\sin(\pi\Delta) \int dt_1 h(t_1) \tilde{K}(t' + t_1 - i\beta/2, r') \tilde{K}^r(t - t_1, r) + (t \leftrightarrow t'), \qquad (3.52)$$

where

$$\tilde{K}(t - t', r) \equiv \langle \phi(t, r) \dot{\phi}(t', \infty) \rangle, \qquad (3.53)$$

$$\tilde{K}^{r}(t-t',r) = |\tilde{K}(t-t',r)|\theta(t)\theta\left(\frac{\sqrt{r^2 - r_0^2}}{r_0}\cosh(t-t') + \frac{r}{r_0}\right), \qquad (3.54)$$

denote a Wightman bulk-to-boundary propagator and a retarded bulk-to-boundary propagator, respectively. The difference with respect to the previous case is that now the propagators involve a source term $\dot{\phi}(t, r = \infty)$ at the boundary, instead than the standard

⁷ Note that $\delta(t-t_0) = -\partial_{t_0}\theta(t-t_0)$, and $\partial_{t_0} = u_0\partial_{u_0}$. This implies that $\Delta v^{\text{inst}} = -u_0\partial_{u_0}\Delta v(u_0)$.

 $\phi(t, r = \infty)$. Other than that, the calculation follows the steps of the case I studied above. Once again, we will carry out the analysis for a general dimension Δ and at the end, we will set $\Delta = 1$.

To start with the calculation we need a propagator of the form

$$\tilde{K}_{\Delta} = \langle \phi_{\mathcal{O}}(r, t) \, \dot{\mathcal{O}}(t') \rangle \,,$$
 (3.55)

where $\phi_{\mathcal{O}}(r,t)$ is the bulk field dual to the operator \mathcal{O} . We can obtain this propagator as

$$\tilde{K}_{\Delta}(t,r;t') = \langle \phi_{\mathcal{O}}(t,r)\,\dot{\mathcal{O}}(t')\rangle = \partial_{t'}\langle \phi_{\mathcal{O}}(t,r)\,\mathcal{O}(t')\rangle = \partial_{t'}K_{\Delta}(t,r;t')\,,\tag{3.56}$$

where $K_{\Delta}(t,r;t') \equiv \langle \phi_{\mathcal{O}}(t,r) \mathcal{O}(t') \rangle$. Using the above identity, we write

$$G_{h} = 2\sin(\pi\Delta) \int dt_{1}h(t_{1})\partial_{t_{1}}K_{\Delta}(t'+t_{1}-i\beta/2,r')\partial_{t_{1}}K_{\Delta}^{r}(t-t_{1},r) + (t\leftrightarrow t'), \quad (3.57)$$

or, in terms of Kruskal coordinates,

$$G_h = \tilde{C}_0 \int \frac{du_1}{u_1} h(u_1) \frac{uu'}{\left(\frac{u}{u_1} - 1\right)^{\Delta + 1} (1 + u'u_1)^{\Delta + 1}} + (u \leftrightarrow u').$$
 (3.58)

Here we used

$$\tilde{K}_{\Delta} = u_1 \partial_{u_1} K_{\Delta} = c_{\Delta} \Delta \frac{u}{u_1} \left[\frac{u}{u_1} - 1 \right]^{-\Delta - 1}, \tag{3.59}$$

$$\tilde{K}_{\Delta}^{r} = u_1 \partial_{u_1} K_{\Delta}^{r} = -c_{\Delta} \Delta u' u_1 \left[u' u_1 + 1 \right]^{-\Delta - 1}, \tag{3.60}$$

where

$$K_{\Delta}(u', 0; -t_1 + i\pi) = c_{\Delta} \left[u'u_1 + 1 \right]^{-\Delta}, \tag{3.61}$$

$$K_{\Delta}^{r}(u,0;t_{1}) = c_{\Delta} \left[\frac{u}{u_{1}} - 1 \right]^{-\Delta}$$
 (3.62)

and $u_1 = e^{t_1}$. Note also that $\partial_{t_1} = u_1 \partial_{u_1}$.

Using $h(u_1) = h \theta(u_1 - u_0)$ and proceeding as for the previous case, we obtain

$$\Delta v = \ell_s^2 h \frac{\pi \Gamma(2\Delta)}{\Gamma(\Delta)^2} (-u_0^{-2})^{1/2 - \Delta} u_0^{1 - 2\Delta} \Delta (1 + \Delta) \left[\Delta B \left(-u_0^{-2}; 1/2 + \Delta, -2\Delta - 2 \right) + 2(1 + \Delta) B \left(-u_0^{-2}; 3/2 + \Delta, -2\Delta - 2 \right) + \Delta B \left(-u_0^{-2}; 5/2 + \Delta, -2\Delta - 2 \right) \right],$$
(3.63)

where B(x; a, b) is the incomplete Beta function. Likewise, the result for an instantaneous perturbation reads

$$\Delta v^{\text{inst}} = -u_0 \partial_{u_0} \Delta v = 2\pi h \ell_s^2 \frac{\Delta(\Delta+1)\Gamma(2\Delta)c_\Delta^2}{\Gamma(\Delta)^2} \frac{u_0^{2\Delta+1}}{(1+u_0^2)^{2\Delta+3}} \left[\Delta - 2(\Delta+1)u_0^2 + \Delta u_0^4 \right].$$
(3.64)

Interestingly, the above result for case II can be obtained from the case I result as follows. First, we consider a slightly more general type I deformation: $\delta H_I = h\phi_L(t_L)\phi_R(t_R)$.

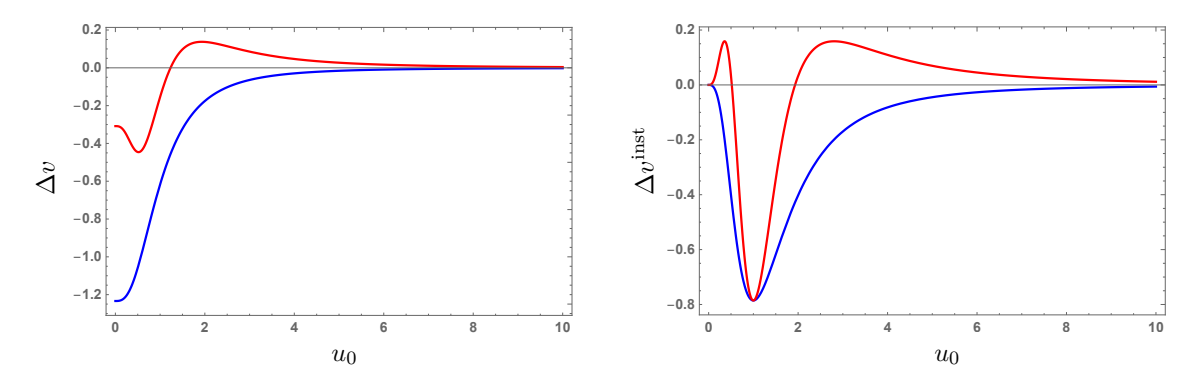


Figure 5. Δv versus $u_0 = e^{t_0}$ for the cases I (blue curves) and II (red curves). Here, we set $h = \ell_s^2 = 1$. We fix $\Delta = 1$ because the double trace deformation involves a massless ϕ , which is dual to a dimension one operator. The left panel shows the result for $h(t) = h\theta(t - t_0)$, while the right panel shows the result for $h(t) = h\delta(t - t_0)$.

Following section 2.2 of [40], we can see that the wormhole opening in this boosted frame reads:⁸

$$\Delta v_I(t_L, t_R) = \frac{\pi c_\Delta^2 \Gamma(2\Delta + 1)}{2^{2+4\Delta} \Gamma(\Delta)^2} \exp\left(-\frac{\pi}{\beta}(t_L + t_R)\right) \left[\frac{1}{2} \cosh\left(\frac{\pi}{\beta}(t_R - t_L)\right)\right]^{-2\Delta - 1}, \quad (3.65)$$

where we have considered that both fields ϕ_L and ϕ_L have dimension Δ . Repeating the same calculation for slightly more general type II perturbations of the form $\delta H_{II} = h\dot{\phi}_L(t_L)\dot{\phi}_R(t_R) = h\partial_{t_L}\partial_{t_R}\phi_L(t_L)\phi_R(t_R)$, it is easy to see that

$$\Delta v_{II}(t_L, t_R) = \partial_{t_L} \partial_{t_R} \Delta v_I(t_L, t_R, \Delta).$$
(3.66)

Similarly, we can check that (3.64) can be obtained as $\partial_{t_L} \partial_{t_R} \Delta v_I(t_L, t_R, \Delta) \big|_{t_R = t_0, t_L = -t_0}$ and using that $u_0 = e^{r_0 t_0}$.

In figure 5, we set $\Delta=1$ and plot Δv as a function of u_0 for type I and type II deformations. The left panel shows the result for a deformation that is turned on at t_0 and remains turned on forever. The right panel shows the result for an instantaneous perturbation. While in case I Δv is negative for any u_0 , in case II Δv is only negative inside some interval $u_0 \in (u_1, u_2)$. In both cases, traversability for an instantaneous perturbation is optimal for $u_0 = 1$, which corresponds to $t_0 = 0$.

3.4 Two-sided commutator

In this section, we will diagnose traversability by sending a signal through the wormhole. The signal is produced by some generic boundary operator W, which is dual to a bulk field ϕ_W . Under certain conditions, the W-quanta traverses the wormhole, producing a non-zero two-sided correlator of the form

$$\langle [W_L(t_L), e^{-i\mathcal{V}}W_R(t_R)e^{i\mathcal{V}}] \rangle$$
, (3.67)

⁸In particular, this expression corresponds to the 2-dimensional version of eq. (2.21) in [40].

where, for the two cases we consider, the double trace deformation is given by

$$V_{\rm I} = \frac{1}{K} \sum_{i=1}^{K} \int dt \, h(t) V_L^i(-t) V_R^i(t) \,, \tag{3.68}$$

$$\mathcal{V}_{\text{II}} = \frac{1}{K} \sum_{i=1}^{K} \int dt \, h(t) \dot{V}_{L}^{i}(-t) \dot{V}_{R}^{i}(t) \,, \tag{3.69}$$

and V^i are boundary operators. We use K different fields because the large-K limit leads to simplifications, e.g., it suppresses particle creation in the worldsheet and enhances the effects of the coupling.⁹ The function h(t) specifies the profile of the deformation. For example, for an instantaneous perturbation that is turned on at time $t = t_0$, we use $h(t) = h \delta(t - t_0)$. The Gao-Jafferis-Wall setup is obtained when we use a Heaviside step function, i.e., $h(t) = h \theta(t - t_0)$.

Taking W and V^i as Hermitian operators, we can write

$$\langle [W_L(t_L), e^{-i\mathcal{V}} W_R(t_R) e^{i\mathcal{V}}] \rangle = -2i \operatorname{Im} C, \qquad (3.70)$$

where

$$C = \langle e^{-i\mathcal{V}} W_R(t_R) e^{i\mathcal{V}} W_L(t_L) \rangle. \tag{3.71}$$

In the large-K and small- ℓ_s limit, we can write [23]

$$C = e^{-i\langle V \rangle} \tilde{C}, \quad \tilde{C} = \langle W_R(t_R) e^{-iV} W_L(t_L) \rangle.$$
 (3.72)

In the following, we will consider the two cases separately.

Case I. Let us start by considering a deformation of case I. Using the eikonal approximation, we can write \tilde{C} as

$$\tilde{C} = \alpha \int dp^u p^u \psi_2^*(p^u) \psi_3(p^u) e^{iD} , \qquad (3.73)$$

with

$$D = \alpha \int dt \, h(t) \int dp^{\nu} p^{\nu} \psi_1^*(p^{\nu}) \psi_4(p^{\nu}) \, e^{i\delta(p^{\mu}p^{\nu})} \,, \tag{3.74}$$

and $\alpha = \frac{4}{\pi r_0}$. The wave functions ψ_i are given by

$$\psi_1(p^v) = \int du e^{2ip^v u} \langle \phi_V(u, v) V_L(-t) \rangle|_{v=0}, \tag{3.75}$$

$$\psi_2(p^u) = \int dv e^{2ip^u v} \langle \phi_W(u, v) W_R(t_R) \rangle|_{u=0}, \tag{3.76}$$

$$\psi_3(p^u) = \int dv e^{2ip^u v} \langle \phi_W(u, v) W_L(t_L) \rangle|_{u=0}, \tag{3.77}$$

$$\psi_4(p^v) = \int du e^{2ip^v u} \langle \phi_V(u, v) V_R(t) \rangle|_{v=0}, \tag{3.78}$$

⁹A concrete suggestion was given in [23] (see appendix C.2. for details). In detail, the idea was to put K strings at the north pole of the S^3 and K oppositely oriented strings at the south pole of S^3 . This is a BPS configuration, related to 1/2 BPS Wilson loops, so it is stable. In general, it is actually rather non-trivial to find microscopic realizations of large K as these typically involve multiple objects with an emergent U(K) gauge symmetry while the non-local deformation is not gauge invariant under this U(K) gauge group.

where ϕ_V and ϕ_W are the bulk fields dual to the operators V and W. The phase shift describing the collision between the W-quanta and the V-quanta reads

$$\delta(p^u p^v) = \ell_s^2 p^u p^v \,. \tag{3.79}$$

The bulk-to-boundary propagators for generic scalar operators are given by

$$\langle \phi_V(u,v)V(t)\rangle = c_{\Delta_V} \left[\frac{1+uv}{ve^t - ue^{-t} + (1-uv)} \right]^{\Delta_V}, \tag{3.80}$$

$$\langle \phi_W(u,v)W(t)\rangle = c_{\Delta_W} \left[\frac{1+uv}{ve^t - ue^{-t} + (1-uv)} \right]^{\Delta_W}, \tag{3.81}$$

where we assume that both (u, v) and t are points on the right-exterior region of the geometry. Fields on the left-exterior region can be obtained by replacing $t \to t + i\frac{\beta}{2}$ in the above formulas. The metric is $ds^2 = 4dudv/(1+uv)^2$. In Schwarzschild coordinates, the horizon radius is r_0 .

After performing the above integrals, we obtain

$$\psi_1 = 2^{\Delta_V} \frac{\pi r_0^{\Delta_V} e^{i\pi \Delta_V/2}}{\Gamma(\Delta_V)} e^{-r_0 t \Delta_V} e^{-2ip^v e^{-r_0 t}} \theta(p^v) (p^v)^{\Delta_V - 1}, \qquad (3.82)$$

$$\psi_2 = 2^{\Delta_W} \frac{\pi r_0^{\Delta_W} e^{i\pi\Delta_W/2}}{\Gamma(\Delta_W)} e^{-r_0 t_R \Delta_W} e^{-2ip^u e^{-r_0 t_R}} \theta(p^u) (p^u)^{\Delta_W - 1}, \qquad (3.83)$$

$$\psi_3 = 2^{\Delta_W} \frac{\pi r_0^{\Delta_W} e^{-i\pi\Delta_W/2}}{\Gamma(\Delta_W)} e^{-r_0 t_L \Delta_W} e^{-2ip^u e^{-r_0 t_L}} \theta(p^u) (p^u)^{\Delta_W - 1}, \qquad (3.84)$$

$$\psi_4 = 2^{\Delta_V} \frac{\pi r_0^{\Delta_V} e^{-i\pi\Delta_V/2}}{\Gamma(\Delta_V)} e^{r_0 t \Delta_V} e^{2ip^v e^{r_0 t}} \theta(p^v) (p^v)^{\Delta_V - 1}.$$
(3.85)

Let us now compute D. Using the above wave functions, we obtain

$$D = \alpha \int dt \, h(t) \int dp^{v} p^{v} \psi_{1}^{*}(p^{v}) \psi_{4}(p^{v}) \, e^{i\delta(p^{u}p^{v})} \,,$$

$$= \alpha_{V} \int dt \, h(t) \int dp^{v} (p^{v})^{2\Delta_{V} - 1} e^{4ip^{v} \cosh(r_{0}t)} e^{i\ell_{s}^{2} p^{u} p^{v}} \,,$$

$$= \alpha_{V} \Gamma(2\Delta_{V}) e^{i\pi\Delta_{V}} \int dt \, h(t) \left[4 \cosh(r_{0}t) + \ell_{s}^{2} p^{u} \right]^{-2\Delta_{V}} \,, \tag{3.86}$$

where $\alpha_V = \pi^2 \alpha 2^{2\Delta_V} \frac{r_0^{2\Delta_V} e^{-i\pi\Delta_V}}{\Gamma(\Delta_V)^2} c_{\Delta_V}^2$ and we used that $\int dp p^{2\Delta-1} e^{ipF} = \Gamma(2\Delta) e^{i\pi\Delta} F^{-2\Delta}$, which is valid when Im(F) > 0.¹⁰

The correlator \tilde{C} can then be written as

$$\tilde{C} = \alpha_W e^{-r_0 \Delta_W (t_L + t_R)} \int dp^u (p^u)^{2\Delta_W - 1} e^{2ip^u \left[e^{-r_0 t_L} + e^{-r_0 t_R} \right]} e^{i\alpha_V \Gamma(2\Delta_V) e^{i\pi\Delta_V}} \int dt \, h(t) \left[4\cosh(r_0 t) + \ell_s^2 p^u \right]^{-2\Delta_V}, \tag{3.87}$$

 $^{^{10}}$ This condition can be satisfied by giving a small imaginary piece to t.

where $\alpha_W = \pi^2 \alpha 2^{2\Delta_W} \frac{r_0^{2\Delta_W} e^{-i\pi\Delta_W}}{\Gamma(\Delta_W)^2} c_{\Delta_W}^2$. For simplicity, let us consider the case in which $h(t) = h r_0^{1-2\Delta} \delta(t-t_0)$. In this case, \tilde{C} becomes

$$\tilde{C} = \alpha_W e^{-r_0 \Delta_W (t_L + t_R)}$$

$$\int dp^u (p^u)^{2\Delta_W - 1} e^{2ip^u \left[e^{-r_0 t_L} + e^{-r_0 t_R} \right]} e^{i\alpha_V \Gamma(2\Delta_V) e^{i\pi\Delta_V} h r_0^{1-2\Delta} \left[4\cosh(r_0 t_0) + \ell_s^2 p^u \right]^{-2\Delta_V}} .$$
(3.88)

The expectation value $\langle \mathcal{V} \rangle$ is obtained from D with $\delta = 0$, i.e.,

$$\langle \mathcal{V} \rangle = D|_{\delta=0} = h r_0^{1-2\Delta} \alpha_V \Gamma(2\Delta_V) e^{i\pi\Delta_V} \left[4\cosh(r_0 t_0) \right]^{-2\Delta_V} . \tag{3.89}$$

We then obtain

$$\tilde{C} = \alpha_W e^{-r_0 \Delta_W (t_L + t_R)} \int dp^u (p^u)^{2\Delta_W - 1} e^{2ip^u \left[e^{-r_0 t_L} + e^{-r_0 t_R} \right]} e^{i\langle \mathcal{V} \rangle \left[1 + \frac{\ell_s^2 p^u}{4 \cosh(r_0 t_0)} \right]^{-2\Delta_V}}, \quad (3.90)$$

and

$$C = e^{-i\langle \mathcal{V} \rangle} \tilde{C}$$

$$= \alpha_W e^{-r_0 \Delta_W (t_L + t_R)} \int_0^\infty dp^u (p^u)^{2\Delta_W - 1} e^{2ip^u \left[e^{-r_0 t_L} + e^{-r_0 t_R}\right]} e^{i\langle \mathcal{V} \rangle \left[\left(1 + \frac{\ell_s^2 p^u}{4 \cosh(r_0 t_0)}\right)^{-2\Delta_V} - 1\right]}.$$
(3.91)

We can study (3.91) numerically to understand the properties of C, but it is also possible to obtain a closed analytic result in the probe approximation, which is obtained by considering a small- p^u approximation, i.e., we consider $D = D_0 + D_1 p^u$, where $D_0 = \langle \mathcal{V} \rangle$:

$$C_{\text{probe}} = \alpha_W e^{-r_0 \Delta_W (t_L + t_R)} \int_0^\infty dp^u (p^u)^{2\Delta_W - 1} e^{2ip^u \left[e^{-r_0 t_L} + e^{-r_0 t_R} \right]} e^{2ip^u \left[-\frac{\langle \mathcal{V} \rangle \Delta_V e^{i\pi \Delta_V \ell_s^2}}{4 \cosh(r_0 t_0)} \right]},$$

$$= \alpha_W e^{-r_0 \Delta_W (t_L + t_R)} \Gamma(2\Delta_W) e^{i\pi \Delta_W} \left[2 \left(e^{-r_0 t_L} + e^{-r_0 t_R} \right) + D_1 \right]^{-2\Delta_W}, \qquad (3.92)$$

where

$$D_{1} = -\frac{2hr_{0}^{1-2\Delta}\alpha_{V}\Delta_{V}\Gamma(2\Delta_{V})e^{i\pi\Delta_{V}}\ell_{s}^{2}}{(4\cosh(r_{0}t_{0}))^{2\Delta_{V}+1}}c_{\Delta_{V}}^{2}.$$
(3.93)

Using the definitions of α , α_W and α_W , we can write

$$C_{\text{probe}} = \pi 2^{2\Delta_W + 2} c_{\Delta_W}^2 \frac{r_0^{2\Delta_W - 1} \Gamma(2\Delta_W)}{\Gamma(\Delta_W)^2} \left[4 \cosh\left(r_0 \frac{t_L - t_R}{2}\right) + D_1 e^{r_0 \frac{t_R + t_L}{2}} \right]^{-2\Delta_W}, \quad (3.94)$$

and

$$D_1 = -2\pi h \frac{\Gamma(2\Delta_V + 1)}{\Gamma(\Delta_V)^2} \frac{\ell_s^2 c_{\Delta_V}^2}{(2\cosh r_0 t_0)^{2\Delta_V + 1}},$$
(3.95)

where we use that $x\Gamma(x) = \Gamma(x+1)$. The deformation changes the geodesic distance between the boundary points t_L and t_R , and its effect is encoded in the term $D_1e^{r_0\frac{t_R+t_L}{2}}$. The term D_1 corresponds to a null shift in the v direction, i.e., $D_1 = 2\Delta v$.

Using that $u_0 = e^{r_0 t_0}$, the above result can be written as

$$\Delta v = \frac{D_1}{2} = -\pi h \frac{\Gamma(2\Delta_V + 1)}{\Gamma(\Delta_V)^2} \frac{\ell_s^2 c_{\Delta_V}^2}{(2\cosh r_0 t_0)^{2\Delta_V + 1}},$$
(3.96)

$$= -\pi h \frac{\Gamma(2\Delta_V + 1)}{\Gamma(\Delta_V)^2} \ell_s^2 c_{\Delta_V}^2 \left(\frac{u_0}{u_0^2 + 1}\right)^{2\Delta_V + 1} , \qquad (3.97)$$

which perfectly agrees with the result (3.51) obtained via point-splitting for case I.

Case II. Let us now compute the two-sided correlator for the second type of perturbation, which involves time derivatives of the boundary operators. We first compute D as

$$D = \alpha \int dt h(t) \int dp^v p^v \tilde{\psi}_1^*(p^v) \tilde{\psi}_4(p^v) e^{i\delta}, \qquad (3.98)$$

where $\tilde{\psi}$ is the Fourier transform of \tilde{K} . These wave functions are obtained as

$$\tilde{\psi}_{1}(p^{v}) = \int du e^{2ip^{v}} \tilde{K}(u,0;t) = \int du e^{2ip^{v}} \partial_{t_{1}} K(u,0;t) = \partial_{t} \psi_{1}(p^{v}) \qquad (3.99)$$

$$= i2^{\Delta_{V}} c_{\Delta_{V}}^{2} \frac{\pi r_{0}^{\Delta_{V}+1} e^{i\pi\Delta_{V}/2}}{\Gamma(\Delta_{V})} e^{-r_{0}t\Delta_{V}} e^{-2ip^{v}e^{-r_{0}t}} \theta(p^{v})(p^{v})^{\Delta_{V}-1} (2ip^{v}e^{-r_{0}t} - \Delta_{V}),$$

$$\tilde{\psi}_{4}(p^{v}) = i2^{\Delta_{V}} c_{\Delta_{V}}^{2} \frac{\pi r_{0}^{\Delta_{V}+1} e^{-i\pi\Delta_{V}/2}}{\Gamma(\Delta_{V})} e^{r_{0}t\Delta_{V}} e^{2ip^{v}e^{r_{0}t}} \theta(p^{v})(p^{v})^{\Delta_{V}-1} (2ip^{v}e^{r_{0}t} + \Delta_{V}). \quad (3.100)$$

For simplicity, we set $r_0 = 1$ and consider an instantaneous perturbation $h(t) = h\delta(t - t_0)$. Using the above wave functions and $\delta = \ell_s^2 p^u p^v$, we can write

$$D = -\frac{2}{\pi} h c_{\Delta_V}^2 2^{2\Delta_V} \frac{\pi^2}{\Gamma(\Delta_V)^2} e^{i\pi\Delta_V}$$

$$\int dp^v (p^v)^{2\Delta_V - 1} e^{4ip^v \cosh t_0} e^{i\ell_s^2 p^u p^v} (2ip^v e^{r_0 t} + \Delta_V) (-2ip^v e^{r_0 t} - \Delta_V)$$

$$= -h4^{\Delta_V + 1} \pi \frac{\Delta_V \Gamma(2\Delta_V)}{\Gamma(\Delta_V)^2} \frac{\left[8 + (8 + \ell_s^4 p^{u^2}) \Delta_V - 8\Delta_V \cosh(2t_0)\right]}{(4 \cosh t_0 + \ell_s^2 p^u)^{2\Delta_V + 2}}.$$
(3.101)

Having obtained D, we can compute the expectation value $\langle \mathcal{V} \rangle$ as

$$\langle \mathcal{V} \rangle = D|_{\delta=0} = \frac{2^{1-2\Delta_V} h \pi \Delta_V}{(\cosh t_0)^{2\Delta_V}} \frac{\Gamma(2\Delta_V)}{\Gamma(\Delta_V)^2} \left[\Delta_V \cosh(2t_0) - \Delta_V - 1 \right] \operatorname{sech}(t_0)^2. \tag{3.102}$$

We can then compute the two-sided commutator as

$$C = e^{-i\langle \mathcal{V} \rangle} \tilde{C}$$

$$= \alpha_W e^{-\Delta_W(t_L + t_R)} \int_0^\infty dp p^{2\Delta_W - 1} e^{2ip\left(e^{-t_L} + e^{-t_R}\right)} e^{\langle \mathcal{V} \rangle} \left[\frac{\left(1 + \frac{\Delta_V \ell_s^4 p^{u_2}}{8[1 + \Delta_V - \Delta_V \cosh(2t_0)]}\right)}{\left(1 + \frac{\ell_s^2 p^u}{4 \cosh t_0}\right)^{2\Delta_V + 2}} - 1 \right]. \tag{3.103}$$

The above expression can be used to study the behavior of C numerically. Before doing that, let us first study C in the probe limit, where we perform a small- p^u approximation, $D = D_0 + D_1 p^u$, with $D_0 = \langle \mathcal{V} \rangle$. We first write

$$C_{\text{probe}} = \alpha_W e^{-\Delta_W (t_L + t_R)} \int_0^\infty dp p^{2\Delta_W - 1} e^{2ip(e^{-t_L} + e^{-t_R})} e^{D_1 p^u}, \qquad (3.104)$$

where

$$D_{1} = -4h\ell_{s}^{2}c_{\Delta_{V}}^{2} \frac{\pi^{2\Delta_{V}}}{\Gamma(\Delta_{V})^{2}} \frac{(\Delta_{V}+1)\Gamma(2\Delta_{V}+1)}{(4\cosh t_{0})^{2\Delta_{V}+3}} \left(8 - 16\Delta\sinh^{2}t_{0}\right),$$

$$= 4\pi\ell_{s}^{2}h \frac{\Gamma(2\Delta_{V})\Delta_{V}(\Delta_{V}+1)}{\Gamma(\Delta_{V})^{2}}c_{\Delta_{V}}^{2} \frac{u_{0}^{2\Delta_{V}+1}}{(1+u_{0}^{2})^{2\Delta_{V}+3}} \left[2u_{0}^{2}(\Delta_{V}+1) - \Delta_{V}u_{0}^{4} - \Delta_{V}\right],$$
(3.105)

and $u_0 = e^{t_0}$. Performing the integral in p^u in (3.104), we find

$$C_{\text{probe}} = \frac{4\pi\Gamma(2\Delta_W)}{\Gamma(\Delta_W)^2} c_{\Delta_W}^2 \left[2\cosh\left(\frac{t_L - t_R}{2}\right) + \frac{D_1}{2} e^{\frac{t_R + t_L}{2}} \right]^{-2\Delta_W}, \tag{3.106}$$

which has the same form as the two-sided commutator for case I, with the only difference that now D_1 is given by (3.105). From D_1 , we can extract the wormhole opening as

$$\Delta v = \frac{D_1}{2} = 2\pi \ell_s^2 h \frac{\Gamma(2\Delta_V)\Delta_V(\Delta_V + 1)}{\Gamma(\Delta_V)^2} c_{\Delta_V}^2 \frac{u_0^{2\Delta_V + 1}}{\left(1 + u_0^2\right)^{2\Delta_V + 3}} \left[2u_0^2(\Delta_V + 1) - \Delta_V u_0^4 - \Delta_V \right], \tag{3.107}$$

which perfectly matches the result obtained via point splitting (3.64).

Note that $\operatorname{Im}(C_{\operatorname{probe}}) = 0$ for integer values of Δ_W , both for (3.94) and (3.106). This implies that, in the probe limit, we cannot send a message through the wormhole using ϕ or $\dot{\phi}$ as the signal. This is an artifact of the probe limit. We will see in the next section that is possible to obtain $\operatorname{Im}(C) \neq 0$ if we include backreaction effects.

3.4.1 Going beyond the probe approximation

In this section, we consider the first corrections beyond the probe approximation. We first note that the commutator given in (3.91) or (3.103) has the form

$$C = \alpha_W \int_0^\infty dP P^{2\Delta_W - 1} e^{4iP} e^{i(D(P) - D_0)}, \qquad (3.108)$$

where we have set $r_0 = 1$, $c_{\Delta_V} = c_{\Delta_W} = 1$ and $t_R = t_L = t$, and defined $P \equiv p^u e^{-t}$.

We now expand D(P) as

$$D(P) = D_0 + D_1 P + D_2 P^2 + \cdots (3.109)$$

The piece $D_0 + D_1 P$ gives the probe limit result, while $D_2 P^2$ takes into account the first effects of backreaction. Substituting (3.109) into (3.108) and performing the integral over P, we obtain

$$C = \alpha_W \frac{(-iD_2)^{\Delta_W}}{2} \left[\Gamma(\Delta_W) \, {}_1F_1 \left(\Delta_W, 1/2, -i\frac{(4+D_1)^2}{4D_2} \right) + \frac{(4+D_1)D_2}{(-iD_2)^{3/2}} \, \Gamma(\Delta_W + 1/2) \, {}_1F_1 \left(\Delta_W + 1/2, 3/2, -i\frac{(4+D_1)^2}{4D_2} \right) \right]. \quad (3.110)$$

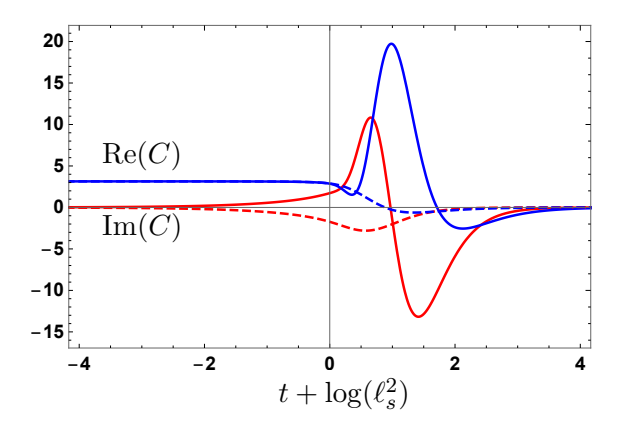


Figure 6. Re(C) (in blue) and Im(C) (in red) versus $t + \log(\ell_s^2)$. The continuous (dashed) curves represent case I (II). Here we set h = 0.6, $\Delta_V = \Delta_W = 1$ and $t_0 = 0$.

After specifying D_1 and D_2 for deformations of the cases I and II, the above equation can be used to study the time-dependence of the commutator.¹¹ Figure 6 shows the real and imaginary part of the commutator C obtained with (3.110).

Now we study the full two-sided commutator by numerically evaluating the integrals (3.91) for case I and (3.103) for case II. In both cases, we set $r_0 = 1$, $c_{\Delta_V} = c_{\Delta_W} = 1$ and $t_R = t_L = t$. By introducing $P = p^u e^{-t}$, the expressions for the two-sided correlators become

$$C_{\rm I} = \alpha_W \int_0^\infty dP P^{2\Delta_W - 1} e^{4iP} e^{iD_0 \left[(1 + \frac{\ell_s^2 P e^t}{4 \cosh t_0})^{-2\Delta_V - 1} \right]},$$

$$D_0 = 4\pi h \frac{\Gamma(2\Delta_V)}{\Gamma(\Delta_V)^2} \left[2 \cosh(t_0) \right]^{-2\Delta_V},$$
(3.111)

and

$$C_{\text{II}} = \alpha_W \int_0^\infty dP P^{2\Delta_W - 1} e^{4iP} e^{iD_0 \left[\left(1 + \frac{\ell_s^2 P e^t}{4 \cosh t_0} \right)^{-2\Delta_V} \left(1 + \frac{\Delta_V \ell_s^4 P^2 e^{2t}}{8[1 + \Delta_V - \Delta_V \cosh(2t_0)]} \right) - 1 \right]},$$

$$D_0 = \frac{2\pi h \Delta_V}{(2\cosh t_0)^{2\Delta_V}} \frac{\Gamma(2\Delta_V)}{\Gamma(\Delta_V)^2} \left[\Delta_V \cosh(2t_0) - \Delta_V - 1 \right] \operatorname{sech}(t_0)^2, \tag{3.112}$$

respectively.

3.4.2 Irrelevant deformations and imprint on the UV

The double trace deformation (3.68) is relevant for $\Delta_V \leq 1/2$. Since we are taking $V = \phi$ or $V = \dot{\phi}$, and ϕ is a massless field, this condition is not satisfied in our setup, and therefore the deformation will have a large imprint on the near boundary geometry. This could explain why in certain cases, the result for the commutator C explodes as one considers high-P contributions of the signal. In fact, insights coming from 2d dilaton gravities and $T\bar{T}$ -deformed theories suggest that one of the leading effects of the irrelevant deformation

¹¹Note that D_1 and D_2 are functions of t.

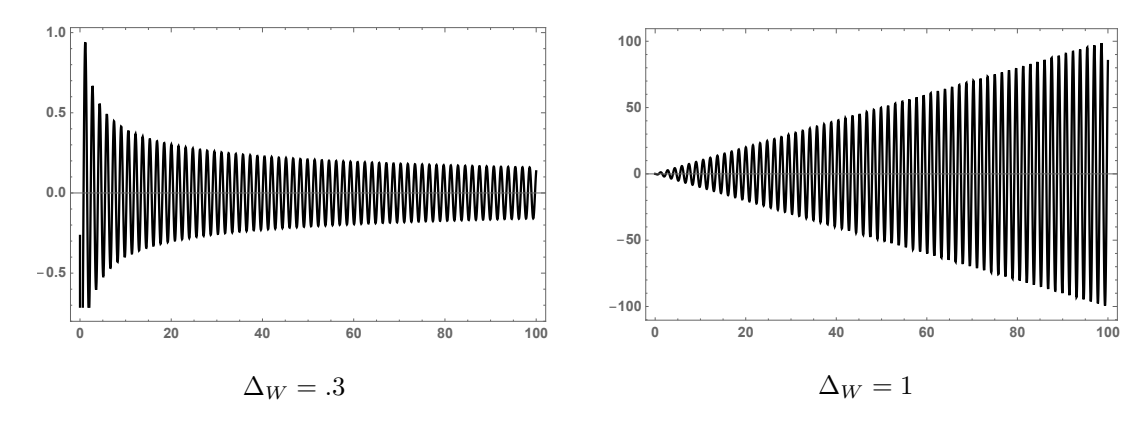


Figure 7. Integrand of $C = \alpha_W \int_0^\infty dP P^{2\Delta_W - 1} e^{4iP} e^{i(D(P) - D_0)}$ as a function of P for $\Delta_W < 1/2$ (left panel) and $\Delta_W > 1/2$ (right panel). Here we consider a deformation of case I and we set $\Delta_V = 1$, $\ell_s = h = c_V = c_W = 1$, $t_0 = 0$ and t = 5.

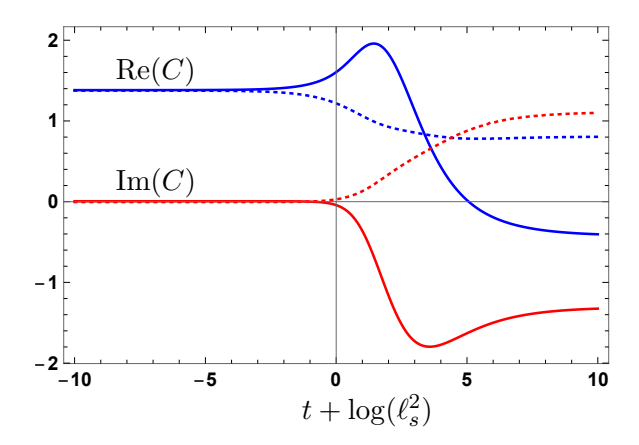


Figure 8. Re(C) (in blue) and Im(C) (in red) versus $t + \log(\ell_s^2)$. The continuous (dashed) curves represent case I (II). Here we set h = 0.6, $\Delta_V = 1$, $\Delta_W = 0.3$ and $t_0 = 0$.

may be the introduction of a natural UV cutoff scale that could cap off the problematic high-P modes.

To analyze this problem in more detail, we will simply introduce a UV cutoff in our calculation, and study its imprint on the observables to determine under what conditions our results are reliable. We introduce a UV cutoff by defining a maximal value r_c for the AdS radial coordinate r.¹² See figure 9. Once we introduce this cutoff, we need rederive our bulk-to-boundary propagators K since they were obtained for a spacetime with boundary at $r \to \infty$. We start by writing the expression for bulk-to-bulk propagators of a scalar field

$$G_{\Delta}(t,r;t',r') = c_{\Delta}\xi^{\Delta}{}_{2}F_{1}\left(\frac{\Delta}{2},\frac{\Delta+1}{2},\Delta+\frac{1}{2};\xi^{2}\right),$$
 (3.113)

$$\xi = \left[-\sqrt{\frac{r^2}{r_0^2} - 1} \sqrt{\frac{r'^2}{r_0^2} - 1} \cosh \frac{r_0(t - t')}{\ell^2} + \frac{rr'}{r_0^2} \right]^{-1}, \quad (3.114)$$

¹²This cutoff can be naturally identified as the position where the flavor branes end.

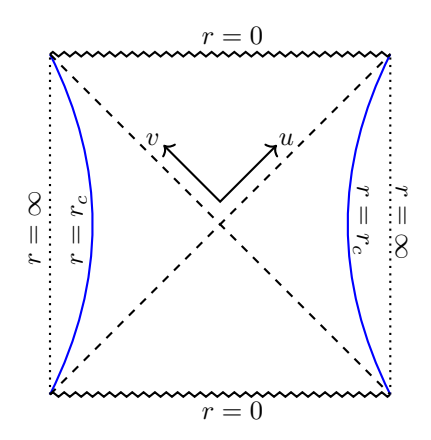


Figure 9. Two-sided AdS black hole with a cutoff at $r = r_c$. The region near the asymptotic boundary at $r = \infty$ is removed, and the geometry ends at the cutoff surface (shown in blue) defined by $r = r_c$.

which is not affected by the presence of the cutoff. Now, we compute the bulk-to-boundary propagator as

$$K_{c}(t,r;t',r_{c}) = \lim_{r'\to r_{c}} r_{c}^{\Delta}G(t,r;t',r')$$

$$= c_{\Delta} \left[-\sqrt{\frac{r^{2}-1}{r_{0}^{2}-1}} \sqrt{r_{0}^{-2}-r_{c}^{-2}} \cosh \frac{r_{0}(t-t')}{\ell^{2}} + \frac{r}{r_{0}^{2}} \right]^{-\Delta} {}_{2}F_{1}\left(\frac{\Delta}{2}, \frac{\Delta+1}{2}, \Delta+\frac{1}{2}; \xi_{c}^{2}\right),$$
(3.115)

where

$$\xi_c = \frac{r_0}{r_c} \left[-\sqrt{\frac{r^2}{r_0^2} - 1} \sqrt{1 - \frac{r_0^2}{r_c^2}} \cosh \frac{r_0(t - t')}{\ell^2} + \frac{r}{r_0} \right]^{-1}.$$
 (3.116)

The strategy now is to compute the wormhole opening Δv in terms of the propagator (3.115) and study how the cutoff affects this quantity.

In Kruskal coordinates, K_c can be written as

$$K_c(u, v; t_1) = c_{\Delta} \left[\frac{1 + uv}{\sqrt{1 - \eta^2} (ve^{r_0 t_1/\ell^2} - ue^{-r_0 t_1/\ell^2}) + 1 - uv} \right]^{\Delta} {}_{2}F_1\left(\frac{\Delta}{2}, \frac{\Delta + 1}{2}, \Delta + \frac{1}{2}; \xi_c^2\right),$$
(3.117)

with

$$\xi_c = \eta \left[\frac{1 + uv}{\sqrt{1 - \eta^2} (ve^{r_0 t_1/\ell^2} - ue^{-r_0 t_1/\ell^2}) + 1 - uv} \right],$$
(3.118)

and $\eta = \frac{r_0}{r}$

Let us first study the effect of the UV cutoff on D, defined in (3.74). We start by writing D in position space

$$D(p^{u}) = \alpha \int dt_{1} h(t_{1}) \int dp^{v} p^{v} \tilde{\psi}_{1}^{*}(p^{v}) \tilde{\psi}_{4}(p^{v}) e^{i\ell_{s}^{2} p^{v} p^{u}}, \qquad (3.119)$$

$$= \alpha \frac{\pi i}{2} \int \frac{du_1}{u_1} h(u_1) \int du K_1^*(u,0;t) \partial_u K_4 \left(u - \frac{\ell_s^2}{2} p^u, 0; t \right) , \qquad (3.120)$$

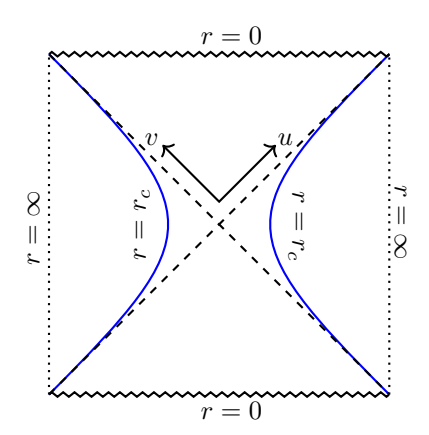


Figure 10. Two-sided AdS black hole with a cutoff at $r = r_c$ very close to the horizon. The region near the asymptotic boundary at $r = \infty$ is removed, and the geometry ends at the cutoff surface (shown in blue) defined by $r = r_c$.

where

$$K_{1}(u,0;u_{1}) = c_{\Delta} \left[\frac{1}{1 - (1 - \eta)\frac{u}{u_{1}}} \right]^{\Delta} {}_{2}F_{1}\left(\frac{\Delta}{2}, \frac{\Delta + 1}{2}, \Delta + \frac{1}{2}; \left[\frac{\eta}{1 - (1 - \eta)\frac{u}{u_{1}}} \right]^{2} \right),$$

$$K_{4}(u - P, 0; u_{1}) = c_{\Delta} \left[\frac{1}{1 - (1 - \eta)\frac{u - P}{u_{1}}} \right]^{\Delta} {}_{2}F_{1}\left(\frac{\Delta}{2}, \frac{\Delta + 1}{2}, \Delta + \frac{1}{2}; \left[\frac{\eta}{1 - (1 - \eta)\frac{u - P}{u_{1}}} \right]^{2} \right),$$

with $P = \frac{\ell_s^2}{2} p^u$, and $u_1 = \sqrt{\frac{r_c - r_0}{r_c + r_0}} e^{r_0 t_1/\ell^2}$. We introduce the variable $U = (1 - \eta)u$, and define

$$k_1(U; u_1) \equiv K_1\left(\frac{U}{1-\eta}, 0; u_1\right) = c_{\Delta} \left[\frac{1}{1-\frac{U}{u_1}}\right]^{\Delta} {}_2F_1\left(\frac{\Delta}{2}, \frac{\Delta+1}{2}, \Delta+\frac{1}{2}; \left[\frac{\eta}{1-\frac{U}{u_1}}\right]^2\right),$$

$$k_4(U; u_1) \equiv K_4\left(\frac{U}{1-\eta}, 0; u_1\right) = c_{\Delta} \left[\frac{1}{1-\frac{U}{u_1}}\right]^{\Delta} {}_2F_1\left(\frac{\Delta}{2}, \frac{\Delta+1}{2}, \Delta+\frac{1}{2}; \left[\frac{\eta}{1-\frac{U}{u_1}}\right]^2\right),$$

in which terms D(P) can be computed as

$$D(P) = \alpha \frac{\pi i}{2} \int \frac{du_1}{u_1} h(u_1) \int dU k_1^*(U, 0; u_1) \partial_U k_4 (U - (1 - \eta)P, 0; u_1) . \tag{3.121}$$

Note that D depends on P through the combination $(1-\eta)P$. Let us now consider a cutoff surface that is located very close to the horizon, such that $\epsilon = (1-\eta) = \frac{r_c - r_0}{r_c}$ is a small parameter. The corresponding Penrose diagram is illustrated in figure 10. In this case, we can expand k_4 in powers of η ,

$$k_4(U - \epsilon P) = k_4(U) + k_4'(U)\epsilon P + k_4''(U)\frac{\epsilon^2 P^2}{2} + \cdots,$$
 (3.122)

and write D as

$$D(P) = D_0 + D_1 \epsilon P + D_2 \epsilon^2 P^2 + \cdots, (3.123)$$

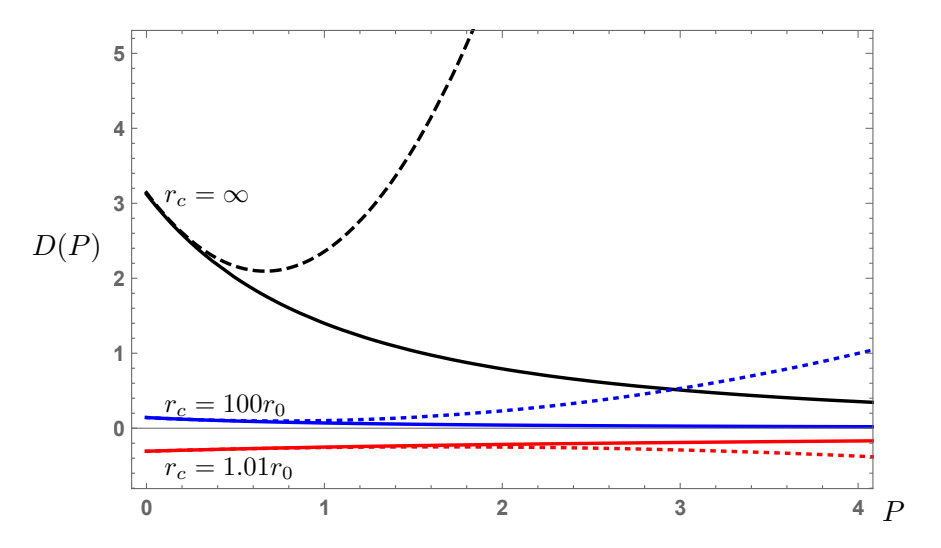


Figure 11. D(P) (continuous lines) as well as $D_0 + D_1P + D_2P^2$ (dotted lines) for different values of the cutoff r_c .

where

$$D_0 = \alpha \frac{\pi i}{2} \int \frac{du_1}{u_1} h(u_1) \int dU k_1^*(U, 0; u_1) \partial_U k_4(U, 0; u_1) , \qquad (3.124)$$

$$D_1 = \alpha \frac{\pi i}{2} \int \frac{du_1}{u_1} h(u_1) \int dU k_1^*(U, 0; u_1) \partial_U^2 k_4(U, 0; u_1) , \qquad (3.125)$$

$$D_2 = \frac{\alpha}{2} \frac{\pi i}{2} \int \frac{du_1}{u_1} h(u_1) \int dU k_1^*(U, 0; u_1) \partial_U^3 k_4(U, 0; u_1) . \tag{3.126}$$

Note that, for very small ϵ , we are very close to the horizon, and we can write $D \approx D_0 + D_1 \epsilon P$, which is very suggestive as it essentially reduces to the probe approximation. As we move the cutoff surface away from the horizon, we need to include higher order terms in (3.121), consistent with the standard notion of UV/IR connection. At second order in ϵP , for example, we obtain the first backreaction effects, which were considered in section 3.4.1. Note that the infinite sum $\sum_{n=0}^{\infty} D_n(\epsilon P)^n$, corresponds to taking the cutoff to the AdS boundary, thus in this case we expect the exact function D(P), which was computed, for example, in (3.86). In this limit, however, the commutator naively diverges, since we are opening the wormhole with an irrelevant double trace deformation and C is therefore very sensitive to the UV physics,

In figure 11, we plot D(P), as well as its second-order approximation $D_0 + D_1 P + D_2 P^2$, for different values of the cutoff r_c . As we could have expected, the plot shows that as we move the cutoff closer and closer to the horizon $(r = r_0)$, the second-order approximation for D(P) becomes more and more precise. On the other hand, for sufficiently large values of P the second-order approximation becomes unreliable, even when r_c is very close to the horizon. We recall that the result from the second-order approximation was already qualitatively similar to the result obtained from smearing the operator, provided P was not too big. So, if we want to guarantee that a small-P approximation is reliable, it is natural to consider a smeared operator but now in the presence of a radial cutoff r_c .

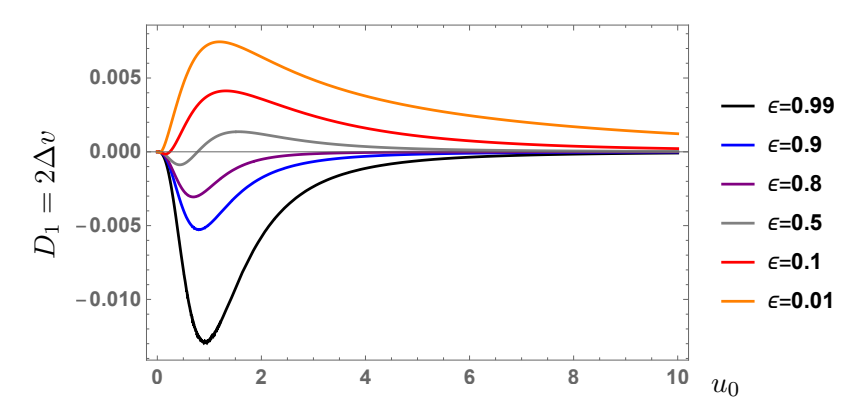


Figure 12. D_1 versus u_0 for different values of the cutoff r_c . Here $\epsilon = 1 - r_0/r_c$, and $\Delta = 1001/1000$. We set $\epsilon = 0.99$ for the black curve, $\epsilon = 0.9$ for the blue curve, $\epsilon = 0.8$ for the purple curve, $\epsilon = 0.5$ for the gray curve, $\epsilon = 0.1$ for the red curve, and $\epsilon = 0.01$ for the orange curve. Even though D_1 becomes positive for small values of ϵ , the worldsheet wormhole can still be made traversable by changing the sign of h.

In figure 12, we plot D_1 vs u_0 for different values of the cutoff r_c . Note that the sign of D_1 changes as we move the cutoff from a position close to the AdS boundary ($r_c = \infty$ or $\epsilon = 1$) to a position close to the horizon ($r_c = r_0$ or $\epsilon = 0$). When $D_1 > 0$, the wormhole can be made traversable by switching the sign of h, which also switches the sign of D_1 .

We now want to study and quantify the effects of the cutoff on the traversability. To do so, we employ a geodesic approximation to compute the two-sided correlator under the presence of a UV cutoff. The basic idea is that the double trace deformation introduces a negative energy in the bulk, which opens the wormhole and shortens the distance between the two asymptotic boundaries. We compute the two-sided correlator as follows [70]

$$\langle W_L(t_L)W_R(t_R)\rangle_h \sim e^{-\Delta_W d(t_L, t_R)},$$
 (3.127)

where $d(t_L, t_R)$ denotes the geodesic distance between the two boundary points, t_L and t_R , and Δ_W is the scaling dimension of the operator W. In the above expression $\langle . \rangle_h$ denotes an expectation value that is taken in the TFD state perturbed by the double trace deformation, i.e., in the presence of a negative energy shock. In embedding coordinates, the geodesic distance d(P, P') between two bulk points $P = (T_1, T_2, X)$ and $P' = (T'_1, T'_2, X')$ is given by

$$\cosh d(P, P') = T_1 T_1' + T_2 T_2' - XX'. \tag{3.128}$$

The embedding coordinates above are related to Kruskal (u, v) and Rindler (t, r) coordinates as follows

$$T_1 = \sqrt{r^2 - 1} \sinh t = \frac{u + v}{1 + uv},$$
 (3.129)

$$T_2 = r = \frac{1 - uv}{1 + uv},\tag{3.130}$$

$$X = \sqrt{r^2 - 1} \cosh t = \frac{v - u}{1 + uv},$$
(3.130)

where we have set $r_0 = 1$. Writing one of the points in Rindler coordinates, and the other in Kruskal coordinates, we find

$$\cosh d(P, P') = \frac{1}{1+uv} \left[\sqrt{r^2 - 1} (ue^t - ue^{-t}) + r(1-uv) \right]. \tag{3.132}$$

Following [71], we write $d = \min_{v}(d_1 + d_2)$, where d_1 (d_2) denotes a distance between the left (right) asymptotic boundary and a point in the u = 0 surface. One can show that

$$d_1 = \operatorname{arccosh}\left(r_c - \sqrt{r_c^2 - 1}e^{-t_L}v\right), \qquad (3.133)$$

$$d_2 = \operatorname{arccosh}\left(r_c + \sqrt{r_c^2 - 1}e^{t_R}(v + \alpha)\right), \qquad (3.134)$$

where α denotes the wormhole opening, and r_c denotes the position of the cutoff. For $t_R = -t_L = t$, one finds that $v_{\min} = -\alpha/2$. The two-sided correlator can then be written as

$$\langle W_L(t_L)W_R(t_R)\rangle_h \sim e^{-\Delta_W(d_1+d_2)}$$

$$= \left[r_c + \frac{1}{2}\left(\alpha e^t \sqrt{r_c^2 - 1} + \sqrt{-2 + 2r_c + e^t \sqrt{r_c^2 - 1}}\sqrt{2 + 2r_c + e^t \sqrt{r_c^2 - 1}}\right)\right]^{-2\Delta_W}.$$
(3.135)

In the limit $r_c \to \infty$, the above result reduces to $(2 + \alpha e^t)^{-2\Delta_W}$ which correspond to the probe limit result C_{probe} obtained in previous sections with $t_R = -t_L = t$, and $\Delta v = \alpha$. This provides evidence that

$$\operatorname{Im}\left(\langle W_L(t_L)W_R(t_R)\rangle_h\right) \sim \langle [W_L(t_L), e^{-i\mathcal{V}}W_R(t_R)e^{i\mathcal{V}}]\rangle. \tag{3.136}$$

Going back to the case with finite r_c , we are interested in determining the time interval for which $\langle W_L(t_L)W_R(t_R)\rangle_h$ has a non-zero imaginary part, especially when we set $\Delta_W = 1$. Studying (3.135), one can show that $\langle W_L(t_L)W_R(t_R)\rangle_h$ becomes complex in the time interval

$$\frac{2}{|\alpha|} \sqrt{\frac{r_c - 1}{r_c + 1}} \le \tilde{t} \le \frac{2}{|\alpha|} \sqrt{\frac{r_c + 1}{r_c - 1}}, \quad \tilde{t} \equiv e^t.$$

$$(3.137)$$

The above interval is centered around $t_c = \log \frac{2}{\alpha}$, which is the time scale that defines a sweet spot for traversability in the absence of a cutoff. The main effect of the cutoff is that now traversability is possible not only at $t = t_c$, but in a time window around t_c that increases as move the cutoff surface deeper into the bulk (i.e., as r_c approaches r_0). See figure 13. Moreover, the above result shows that the commutator is non-zero even when Δ_W takes integer values, which was not the case when $r_c \to \infty$ in the probe approximation.

4 Discussion

In this work, we studied worldsheet wormholes that become traversable after coupling the two endpoints of an open string in AdS. We considered the standard double trace deformation, $\delta \mathcal{L} \sim h \phi_L \phi_R$, introduced by Gao, Jafferis and Wall, as well as a second type of deformation of the form $\delta \mathcal{L} \sim h \partial \phi_L \partial \phi_R$, which seems more natural from the

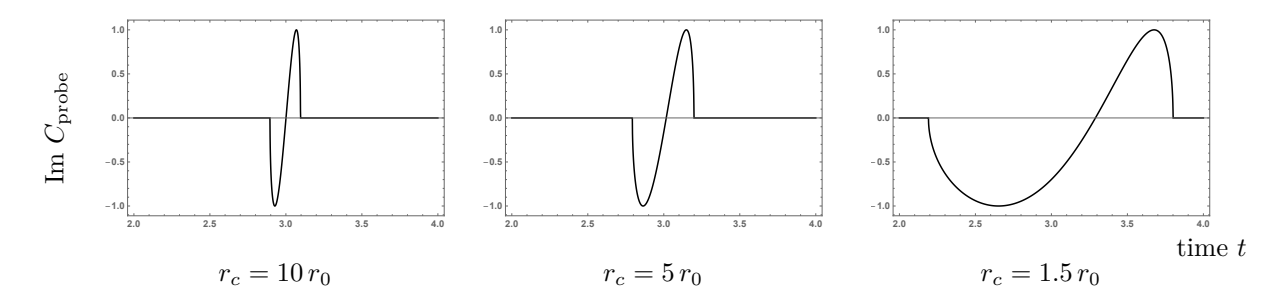


Figure 13. Im $C_{\text{probe}}(t; r_c)$ vs. time t for increasing values of r_c/r_0 . Here we fixed $\alpha = -0.1$ and $\Delta_W = 1$.

worldsheet perspective and could in principle emerge from the interactions between the string endpoints.

Normally, in higher dimensional setups, the traversability of wormholes can be diagnosed from violations of the ANEC, which states that the integral of the stress-energy tensor along complete achronal null geodesics is non-negative. Although this condition is satisfied in any local quantum field theory, the double-trace deformation that is introduced is non-local, invalidating one of the main assumptions of the ANEC and effectively rendering all null geodesics connecting the two boundaries non-achronal. Our two-dimensional setup includes a similar non-local coupling but does not contain gravity in the standard sense, so we needed to come up with a different criterion to check the traversability. In section 3.2, we showed that worldsheet wormholes may indeed become traversable in the presence of worldsheet fluctuations with negative energy. More specifically, we showed that a signal originating in the left asymptotic boundary generally suffers a null shift Δv in its trajectory, which is given by $\Delta v = \Delta E/8$, where ΔE is the energy of worldsheet fluctuations. This means that the signal may only reach the right asymptotic boundary if $\Delta v < 0$, which requires $\Delta E < 0$. This condition is analogous to the ANEC for standard gravitational setups and explains why traversable wormholes cannot arise when considering classical fluctuations of the string [11].

Using the point-splitting method, we computed the wormhole opening for two types of deformations and we found the following results:

Case I:
$$\delta H_{I} = h\delta(t - t_{0})\phi_{L}(-t_{0})\phi_{R}(t_{0})$$

$$\Delta v_{I}^{\text{inst}} = -\frac{h\ell_{s}^{2}}{2\pi} \left(\frac{u_{0}}{1 + u_{0}^{2}}\right)^{3}$$
(4.1)
$$\delta H_{II} = h\delta(t - t_{0})\dot{\phi}_{L}(-t_{0})\dot{\phi}_{R}(t_{0})$$

$$\Delta v_{II}^{\text{inst}} = \frac{h\ell_{s}^{2}}{\pi} \frac{u_{0}^{3}}{(1 + u_{0}^{2})^{5}} \left[1 - 4u_{0}^{2} + u_{0}^{4}\right]$$
(4.2)

Using the eikonal approximation, we then computed the two-sided commutator

$$C(t_L, t_R) = \langle [\phi_L(t_L), e^{-i\mathcal{V}} \phi_R(t_R) e^{i\mathcal{V}}] \rangle$$
(4.3)

where \mathcal{V} is a deformation of type I or II made with a large number of operators, K, defined

as in (3.68) [23].¹³ This commutator measures how effectively we can send a message through the wormhole, displaying a non-zero value when the wormhole is traversable. At the technical level, the calculation mimics the computation of the OTOC [56], except that the operators \mathcal{V} introduce negative energy as opposed to positive energy. Crucial to this calculation is the phase shift $\delta(s)$, which turns out to be linear in the Mandelstam variable $s = (\Delta E)^2$. This linear phase shift is surprising for a theory without dynamical gravitons¹⁴ and was singled out in [56] as responsible for maximal chaos. Our study hints at a more dramatic conclusion: wormhole traversability and maximal chaos go hand in hand, provided there is enough entanglement that can be used as a resource.

Let us now discuss our results. First, we considered the signal in the probe approximation. In this case, the commutator was written in terms of the geodesic distance between the points t_L and t_R on the left and right asymptotic boundaries, respectively. The effect of the deformation of type I (type II) is to introduce null energy in the bulk, which in turn induces a decrease in the geodesic distance by Δv_I (Δv_{II}). This commutator calculation thus provides an alternative way of computing the wormhole opening Δv , which perfectly matched the result obtained by point-splitting. The first backreaction effects of the signal were also obtained analytically. The final result for the commutator with the first-order corrections was displayed in figure 6. We then studied numerically the full backreaction effects of the signal. In this case, however, it was important to consider a smeared version of the signal that suppresses high momentum contributions, since the operator deforming the theory is irrelevant. We analyzed two ways of smearing the operator, one by considering a hard cutoff and another one by adding an exponential damping term. Regardless of the way we cut the high-P contributions, the results obtained were qualitatively similar to the results obtained by considering the first backreaction effects. This implies that the net effect of the irrelevant coupling could be accounted for by cutting off part of the asymptotic boundary, which effectively removes the aforementioned high-P modes. This is in agreement with intuition from 2d dilaton gravity theories, where a similar effect also shows up when considering irrelevant deformations.

We can better understand the effects of the double-trace deformation on the near-boundary geometry if we think of the worldsheet as a $T\bar{T}$ -like deformed theory [60]. The irrelevant deformation introduces a geometric cutoff r_c that removes the asymptotic region of AdS, placing the dual boundary theory on a finite radial distance $r = r_c$ in the bulk [63]. With this interpretation in mind, we studied how the UV cutoff affects our results for the wormhole opening and for the commutator that diagnoses traversability. We observed that the UV cutoff improves the probe approximation and improves the traversability conditions, making it easier to send information through the wormhole. The appearance and value of the cutoff scale r_c may be related to the strength of the irrelevant deformation h. To

 $^{^{13}}$ To achieve this we can consider a system of K non-interacting strings, or a K-string. This approximation is useful because it enhances the effects of the coupling while suppressing particle creation in the worldsheet. However, K cannot be too large, otherwise, interactions between individual strings become relevant. In such cases, a better description of the system is in terms of a D3-brane carrying K units of electric flux [72–74]. It would be interesting to consider traversable wormholes in that setting.

¹⁴The linear shift arises from resummation of all possible higher spin excitations of the string.

see this, notice that in the presence of the deformation, there is a scalar mode that grows near the boundary as $\phi \sim h \, r^{\Delta - d}$, and blows up for $\Delta > d$. To have a controlled theory, we need a UV cutoff such that $h \, r^{\Delta - d} < 1$. As h is increased, we are thus forced to pick smaller values of r_c and eventually, let $r_c \to r_0$. Further, via the standard UV/IR relations in holography, one could map r_c into a momentum scale $r_c \sim P_{\rm max}$ in the dual theory, as part of the UV geometry is capped off. This is in complete agreement with our numerical findings concerning smeared operators.

An interesting future direction regarding worldsheet wormholes is the study of out-of-time-order six-point functions which characterize collisions in the wormhole interior. By introducing a coupling between the two asymptotic boundaries, one can make the world-sheet wormhole traversable and, thus, extract information about the collision product from behind the horizon [75]. Another possible generalization would be to construct traversable wormholes on branes, instead of strings. This could be achieved by considering higher dimensional versions of the solutions used here [76]. In fact, an attribute of worldvolume theories is that they may include dynamical gravity, in a way reminiscent of Randall-Sundrum braneworld models [77, 78]. In these setups, semiclassical backreaction may be treated exactly, i.e., including all orders in the Newton's constant G_N (cf. [79–82]). It would be interesting to investigate how the bounds on information transfer may be affected by semiclassical backreaction in these setups.

Acknowledgments

We are grateful to Jose Barbón, Elena Cáceres, Ben Freivogel, Alberto Güijosa, Arnab Kundu, Kyoungsun Lee, Ayan Patra, and Andrew Svesko for useful discussions and comments on the manuscript. JdB is supported by the European Research Council under the European Unions Seventh Framework Programme (FP7/2007-2013), ERC Grant agreement ADG 834878. VJ and KYK are supported by the National Research Foundation of Korea (NRF) funded by the Ministry of Education and the Ministry of Science, ICT & Future Planning (NRF-2021R1A2C1006791 and NRF-2020R1I1A1A01073135), the GIST Research Institute (GRI) and the AI-based GIST Research Scientist Project grant funded by the GIST in 2023. KYK is also supported by Creation of the Quantum Information Science R&D Ecosystem (Grant No. 2022M3H3A106307411) through the National Research Foundation of Korea (NRF) funded by the Korean government (Ministry of Science and ICT). JFP is supported by the 'Atracción de Talento' program (2020-T1/TIC-20495, Comunidad de Madrid) and by the Spanish Research Agency (Agencia Estatal de Investigación) through the grants CEX2020-001007-S and PID2021-123017NB-I00, funded by MCIN/AEI/10.13039/501100011033 and by ERDF A way of making Europe.

Open Access. This article is distributed under the terms of the Creative Commons Attribution License (CC-BY 4.0), which permits any use, distribution and reproduction in any medium, provided the original author(s) and source are credited. SCOAP³ supports the goals of the International Year of Basic Sciences for Sustainable Development.

References

- [1] A. Einstein and N. Rosen, The Particle Problem in the General Theory of Relativity, Phys. Rev. 48 (1935) 73 [INSPIRE].
- [2] C.W. Misner and J.A. Wheeler, Classical physics as geometry: Gravitation, electromagnetism, unquantized charge, and mass as properties of curved empty space, Annals Phys. 2 (1957) 525 [INSPIRE].
- [3] A.R. Brown et al., Quantum Gravity in the Lab. I. Teleportation by Size and Traversable Wormholes, PRX Quantum 4 (2023) 010320 [arXiv:1911.06314] [INSPIRE].
- [4] S. Nezami et al., Quantum Gravity in the Lab. II. Teleportation by Size and Traversable Wormholes, PRX Quantum 4 (2023) 010321 [arXiv:2102.01064] [INSPIRE].
- [5] J.M. Maldacena, The Large N limit of superconformal field theories and supergravity, Adv. Theor. Math. Phys. 2 (1998) 231 [hep-th/9711200] [INSPIRE].
- [6] J.M. Maldacena, Eternal black holes in anti-de Sitter, JHEP 04 (2003) 021 [hep-th/0106112] [INSPIRE].
- [7] M. Van Raamsdonk, Building up spacetime with quantum entanglement, Gen. Rel. Grav. 42 (2010) 2323 [arXiv:1005.3035] [INSPIRE].
- [8] J. Maldacena and L. Susskind, Cool horizons for entangled black holes, Fortsch. Phys. 61 (2013) 781 [arXiv:1306.0533] [INSPIRE].
- [9] K. Jensen and A. Karch, Holographic Dual of an Einstein-Podolsky-Rosen Pair has a Wormhole, Phys. Rev. Lett. 111 (2013) 211602 [arXiv:1307.1132] [INSPIRE].
- [10] J. Sonner, Holographic Schwinger Effect and the Geometry of Entanglement, Phys. Rev. Lett. 111 (2013) 211603 [arXiv:1307.6850] [INSPIRE].
- [11] M. Chernicoff, A. Güijosa and J.F. Pedraza, *Holographic EPR Pairs*, *Wormholes and Radiation*, *JHEP* **10** (2013) 211 [arXiv:1308.3695] [INSPIRE].
- [12] K. Jensen, A. Karch and B. Robinson, *Holographic dual of a Hawking pair has a wormhole*, *Phys. Rev. D* **90** (2014) 064019 [arXiv:1405.2065] [INSPIRE].
- [13] W. Fischler, P.H. Nguyen, J.F. Pedraza and W. Tangarife, *Holographic Schwinger effect in de Sitter space*, *Phys. Rev. D* **91** (2015) 086015 [arXiv:1411.1787] [INSPIRE].
- [14] V.E. Hubeny and G.W. Semenoff, String worldsheet for accelerating quark, JHEP 10 (2015) 071 [arXiv:1410.1171] [INSPIRE].
- [15] B.-W. Xiao, On the exact solution of the accelerating string in AdS(5) space, Phys. Lett. B 665 (2008) 173 [arXiv:0804.1343] [INSPIRE].
- [16] E. Caceres, M. Chernicoff, A. Guijosa and J.F. Pedraza, Quantum Fluctuations and the Unruh Effect in Strongly-Coupled Conformal Field Theories, JHEP 06 (2010) 078 [arXiv:1003.5332] [INSPIRE].
- [17] A.N. Atmaja, J. de Boer and M. Shigemori, *Holographic Brownian Motion and Time Scales in Strongly Coupled Plasmas*, *Nucl. Phys. B* 880 (2014) 23 [arXiv:1002.2429] [INSPIRE].
- [18] P. Banerjee and B. Sathiapalan, *Holographic Brownian Motion in 1+1 Dimensions*, *Nucl. Phys. B* **884** (2014) 74 [arXiv:1308.3352] [INSPIRE].
- [19] S.H. Shenker and D. Stanford, Stringy effects in scrambling, JHEP **05** (2015) 132 [arXiv:1412.6087] [INSPIRE].

- [20] J. Maldacena, S.H. Shenker and D. Stanford, *A bound on chaos*, *JHEP* **08** (2016) 106 [arXiv:1503.01409] [INSPIRE].
- [21] P. Gao, D.L. Jafferis and A.C. Wall, Traversable Wormholes via a Double Trace Deformation, JHEP 12 (2017) 151 [arXiv:1608.05687] [INSPIRE].
- [22] M. Chernicoff, J.A. Garcia and A. Guijosa, A Tail of a Quark in N=4 SYM, JHEP **09** (2009) 080 [arXiv:0906.1592] [INSPIRE].
- [23] J. Maldacena, D. Stanford and Z. Yang, *Diving into traversable wormholes*, *Fortsch. Phys.* **65** (2017) 1700034 [arXiv:1704.05333] [INSPIRE].
- [24] D. Bak, C. Kim and S.-H. Yi, Bulk view of teleportation and traversable wormholes, JHEP 08 (2018) 140 [arXiv:1805.12349] [INSPIRE].
- [25] D. Bak, C. Kim and S.-H. Yi, Transparentizing Black Holes to Eternal Traversable Wormholes, JHEP 03 (2019) 155 [arXiv:1901.07679] [INSPIRE].
- [26] J. Maldacena, A. Milekhin and F. Popov, *Traversable wormholes in four dimensions*, arXiv:1807.04726 [INSPIRE].
- [27] B. Ahn et al., Holographic teleportation in higher dimensions, JHEP 07 (2021) 219 [arXiv:2011.13807] [INSPIRE].
- [28] B. Ahn, S.-E. Bak, V. Jahnke and K.-Y. Kim, Holographic teleportation with conservation laws: diffusion on traversable wormholes, arXiv:2206.03434 [INSPIRE].
- [29] Z. Fu, B. Grado-White and D. Marolf, Traversable Asymptotically Flat Wormholes with Short Transit Times, Class. Quant. Grav. 36 (2019) 245018 [arXiv:1908.03273] [INSPIRE].
- [30] A. Al Balushi, Z. Wang and D. Marolf, Traversability of Multi-Boundary Wormholes, JHEP 04 (2021) 083 [arXiv:2012.04635] [INSPIRE].
- [31] R. Emparan, B. Grado-White, D. Marolf and M. Tomasevic, *Multi-mouth Traversable Wormholes*, *JHEP* **05** (2021) 032 [arXiv:2012.07821] [INSPIRE].
- [32] J. Maldacena and X.-L. Qi, Eternal traversable wormhole, arXiv:1804.00491 [INSPIRE].
- [33] B. Freivogel et al., Lessons on eternal traversable wormholes in AdS, JHEP 07 (2019) 122 [arXiv:1903.05732] [INSPIRE].
- [34] S. Bintanja, R. Espíndola, B. Freivogel and D. Nikolakopoulou, *How to make traversable wormholes: eternal AdS*₄ *wormholes from coupled CFT's*, *JHEP* **10** (2021) 173 [arXiv:2102.06628] [INSPIRE].
- [35] S. Fallows and S.F. Ross, Making near-extremal wormholes traversable, JHEP 12 (2020) 044 [arXiv:2008.07946] [INSPIRE].
- [36] E. Caceres, A.S. Misobuchi and M.-L. Xiao, Rotating traversable wormholes in AdS, JHEP 12 (2018) 005 [arXiv:1807.07239] [INSPIRE].
- [37] J. Maldacena and A. Milekhin, *Humanly traversable wormholes*, *Phys. Rev. D* **103** (2021) 066007 [arXiv:2008.06618] [INSPIRE].
- [38] A. Almheiri, A. Mousatov and M. Shyani, Escaping the interiors of pure boundary-state black holes, JHEP 02 (2023) 024 [arXiv:1803.04434] [INSPIRE].
- [39] N. Bao, A. Chatwin-Davies, J. Pollack and G.N. Remmen, Traversable Wormholes as Quantum Channels: Exploring CFT Entanglement Structure and Channel Capacity in Holography, JHEP 11 (2018) 071 [arXiv:1808.05963] [INSPIRE].

- [40] B. Freivogel, D.A. Galante, D. Nikolakopoulou and A. Rotundo, *Traversable wormholes in AdS and bounds on information transfer*, *JHEP* **01** (2020) 050 [arXiv:1907.13140] [INSPIRE].
- [41] J. Couch et al., Speed of quantum information spreading in chaotic systems, Phys. Rev. B 102 (2020) 045114 [arXiv:1908.06993] [INSPIRE].
- [42] D. Marolf and S. McBride, Simple Perturbatively Traversable Wormholes from Bulk Fermions, JHEP 11 (2019) 037 [arXiv:1908.03998] [INSPIRE].
- [43] Z. Fu, B. Grado-White and D. Marolf, A perturbative perspective on self-supporting wormholes, Class. Quant. Grav. 36 (2019) 045006 [Erratum ibid. 36 (2019) 249501] [arXiv:1807.07917] [INSPIRE].
- [44] S. Hirano, Y. Lei and S. van Leuven, Information Transfer and Black Hole Evaporation via Traversable BTZ Wormholes, JHEP 09 (2019) 070 [arXiv:1906.10715] [INSPIRE].
- [45] B. Freivogel, D. Nikolakopoulou and A.F. Rotundo, Wormholes from Averaging over States, SciPost Phys. 14 (2023) 026 [arXiv:2105.12771] [INSPIRE].
- [46] H. Geng, Non-local entanglement and fast scrambling in de-Sitter holography, Annals Phys. 426 (2021) 168402 [arXiv:2005.00021] [INSPIRE].
- [47] T. Nosaka and T. Numasawa, Chaos exponents of SYK traversable wormholes, JHEP 02 (2021) 150 [arXiv:2009.10759] [INSPIRE].
- [48] A. Levine, A. Shahbazi-Moghaddam and R.M. Soni, Seeing the entanglement wedge, JHEP 06 (2021) 134 [arXiv:2009.11305] [INSPIRE].
- [49] A.M. García-García, T. Nosaka, D. Rosa and J.J.M. Verbaarschot, Quantum chaos transition in a two-site Sachdev-Ye-Kitaev model dual to an eternal traversable wormhole, Phys. Rev. D 100 (2019) 026002 [arXiv:1901.06031] [INSPIRE].
- [50] T. Numasawa, Four coupled SYK models and nearly AdS₂ gravities: phase transitions in traversable wormholes and in bra-ket wormholes, Class. Quant. Grav. 39 (2022) 084001 [arXiv:2011.12962] [INSPIRE].
- [51] A. Anand and P.K. Tripathy, Self-supporting wormholes with massive vector field, Phys. Rev. D 102 (2020) 126016 [arXiv:2008.10920] [INSPIRE].
- [52] A. Anand, Self-Supporting Wormholes in Four Dimensions with Scalar Field, arXiv:2204.08178 [INSPIRE].
- [53] A. Kundu, Wormholes and holography: an introduction, Eur. Phys. J. C 82 (2022) 447 [arXiv:2110.14958] [INSPIRE].
- [54] S. Dubovsky, R. Flauger and V. Gorbenko, Solving the Simplest Theory of Quantum Gravity, JHEP 09 (2012) 133 [arXiv:1205.6805] [INSPIRE].
- [55] K. Murata, Fast scrambling in holographic Einstein-Podolsky-Rosen pair, JHEP 11 (2017) 049 [arXiv:1708.09493] [INSPIRE].
- [56] J. de Boer, E. Llabrés, J.F. Pedraza and D. Vegh, Chaotic strings in AdS/CFT, Phys. Rev. Lett. 120 (2018) 201604 [arXiv:1709.01052] [INSPIRE].
- [57] A. Banerjee, A. Kundu and R.R. Poojary, Strings, branes, Schwarzian action and maximal chaos, Phys. Lett. B 838 (2023) 137632 [arXiv:1809.02090] [INSPIRE].
- [58] A. Banerjee, A. Kundu and R. Poojary, Maximal Chaos from Strings, Branes and Schwarzian Action, JHEP 06 (2019) 076 [arXiv:1811.04977] [INSPIRE].

- [59] D. Vegh, Celestial fields on the string and the Schwarzian action, JHEP 07 (2021) 050 [arXiv:1910.03610] [INSPIRE].
- [60] A. Cavaglià, S. Negro, I.M. Szécsényi and R. Tateo, TT-deformed 2D Quantum Field Theories, JHEP 10 (2016) 112 [arXiv:1608.05534] [INSPIRE].
- [61] N. Callebaut, J. Kruthoff and H. Verlinde, $T\overline{T}$ deformed CFT as a non-critical string, JHEP 04 (2020) 084 [arXiv:1910.13578] [INSPIRE].
- [62] S. Chakraborty, A. Giveon and D. Kutasov, $T\bar{T}$, $J\bar{T}$, $T\bar{J}$ and String Theory, J. Phys. A 52 (2019) 384003 [arXiv:1905.00051] [INSPIRE].
- [63] L. McGough, M. Mezei and H. Verlinde, Moving the CFT into the bulk with $T\overline{T}$, JHEP 04 (2018) 010 [arXiv:1611.03470] [INSPIRE].
- [64] S. Dubovsky, V. Gorbenko and M. Mirbabayi, Asymptotic fragility, near AdS_2 holography and $T\overline{T}$, JHEP **09** (2017) 136 [arXiv:1706.06604] [INSPIRE].
- [65] P. Kraus, J. Liu and D. Marolf, Cutoff AdS_3 versus the $T\overline{T}$ deformation, JHEP **07** (2018) 027 [arXiv:1801.02714] [INSPIRE].
- [66] C. Ferko and S. Sethi, Sequential Flows by Irrelevant Operators, SciPost Phys. 14 (2023) 098 [arXiv:2206.04787] [INSPIRE].
- [67] A. Karch and E. Katz, Adding flavor to AdS / CFT, JHEP 06 (2002) 043 [hep-th/0205236] [INSPIRE].
- [68] R. Haag, N.M. Hugenholtz and M. Winnink, On the Equilibrium states in quantum statistical mechanics, Commun. Math. Phys. 5 (1967) 215 [INSPIRE].
- [69] P. Gao and H. Liu, Regenesis and quantum traversable wormholes, JHEP 10 (2019) 048 [arXiv:1810.01444] [INSPIRE].
- [70] A.P. Reynolds and S.F. Ross, Butterflies with rotation and charge, Class. Quant. Grav. 33 (2016) 215008 [arXiv:1604.04099] [INSPIRE].
- [71] S.H. Shenker and D. Stanford, Black holes and the butterfly effect, JHEP 03 (2014) 067 [arXiv:1306.0622] [INSPIRE].
- [72] N. Drukker and B. Fiol, All-genus calculation of Wilson loops using D-branes, JHEP 02 (2005) 010 [hep-th/0501109] [INSPIRE].
- [73] J. Gomis and F. Passerini, Wilson Loops as D3-Branes, JHEP 01 (2007) 097 [hep-th/0612022] [INSPIRE].
- [74] B. Fiol, A. Güijosa and J.F. Pedraza, Branes from Light: Embeddings and Energetics for Symmetric k-Quarks in $\mathcal{N}=4$ SYM, JHEP **01** (2015) 149 [arXiv:1410.0692] [INSPIRE].
- [75] F.M. Haehl, A. Streicher and Y. Zhao, Six-point functions and collisions in the black hole interior, JHEP 08 (2021) 134 [arXiv:2105.12755] [INSPIRE].
- [76] M. Arcos, W. Fischler, J.F. Pedraza and A. Svesko, Membrane nucleation rates from holography, JHEP 12 (2022) 141 [arXiv:2207.06447] [INSPIRE].
- [77] L. Randall and R. Sundrum, An Alternative to compactification, Phys. Rev. Lett. 83 (1999) 4690 [hep-th/9906064] [INSPIRE].
- [78] L. Randall and R. Sundrum, A Large mass hierarchy from a small extra dimension, Phys. Rev. Lett. 83 (1999) 3370 [hep-ph/9905221] [INSPIRE].

- [79] R. Emparan, G.T. Horowitz and R.C. Myers, Exact description of black holes on branes, JHEP 01 (2000) 007 [hep-th/9911043] [INSPIRE].
- [80] R. Emparan, A. Fabbri and N. Kaloper, Quantum black holes as holograms in AdS brane worlds, JHEP 08 (2002) 043 [hep-th/0206155] [INSPIRE].
- [81] R. Emparan, A.M. Frassino and B. Way, *Quantum BTZ black hole*, *JHEP* **11** (2020) 137 [arXiv:2007.15999] [INSPIRE].
- [82] R. Emparan et al., Black holes in dS_3 , JHEP 11 (2022) 073 [arXiv:2207.03302] [INSPIRE].